CONFIDENTIAL

OFFICE OF SCIENTIFIC RESEARCH & DEVELOPMENT

NATIONAL DEFENSE RESEARCH COMMITTEE.

DIVISION SIX-SECTION 6.1 RESTRICTED

PRESSURE DISTRIBUTION MEASUREMENTS ON THE MK 13-1, 13-2, AND 13-2A TORPEDOES.

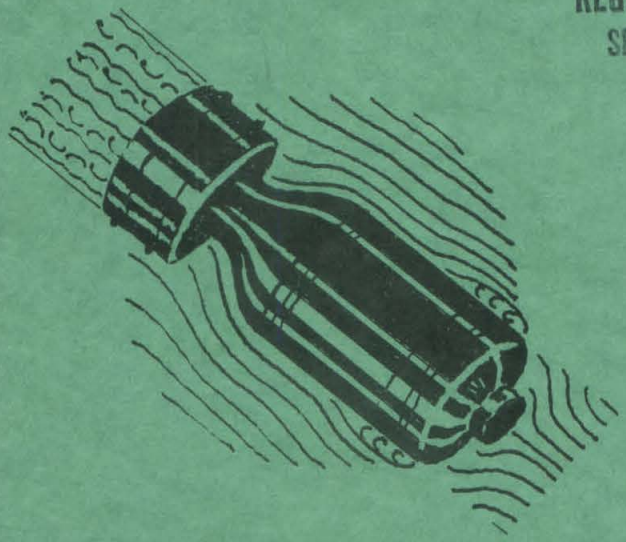

THE HIGH SPEED WATER TUNNEL
CALIFORNIA INSTITUTE OF TECHNOLOGY
PASADENA, CALIFORNIA.

SECTION Nº 6.1 Sr 207-1643
ND-15.3

COPY Nº 102

RESTRICTED

CONFIDENTIAL

OFFICE OF SCIENTIFIC RESEARCH AND DEVELOPMENT
NATIONAL DEFENSE RESEARCH COMMITTEE
DIVISION SIX – SECTION 6.1

PRESSURE DISTRIBUTION MEASUREMENTS ON THE MK 13-1, 13-2, AND 13-2A TORPEDOES

BY

ROBERT T. KNAPP
OFFICIAL INVESTIGATOR

THE HIGH SPEED WATER TUNNEL
AT THE
CALIFORNIA INSTITUTE OF TECHNOLOGY
HYDRAULIC MACHINERY LABORATORY
PASADENA, CALIFORNIA

Section No. 6.1-sr207-1643

HML Rep. No. ND-15.3

Report Prepared by
Joseph Levy
Hydraulic Engineer

June 23, 1944

TABLE OF CONTENTS

ABSTRACT AND SUMMARY

This report includes measurements of the pressure distribution on the body of the Mk 13 torpedo, Modifications 1, 2, and 2A, and shows the effects of variations in yaw and pitch angle, velocity, and static pressure (i.e., submergence). The measurements were made without propellers. The main objective of the investigation was to determine whether or not the depth control mechanism is actuated by true hydrostatic pressure and to determine, if possible, the cause of the erratic depth-keeping behavior of these torpedoes. In addition, the pressure data is applied to discussing the depth and roll recorder performance, to checking cavitation characteristics, and to evaluating forces and moments acting on the projectile. The important observations and conclusions are presented in the following summary:

1. The pressure on the surface of the torpedo equals the static pressure of the undisturbed water ($P = P_o$) at two positions, one on the nose and one on the afterbody (Figure 8). Between these two stations (approximately 82% of the body length), the pressure is below static.

2. The position for $P = P_o$ on the afterbody depends on the proximity of the fins, being slightly farther forward near the fins (Figure 22, Station 19).

3. The position for $P = P_o$ on the afterbody is only slightly affected by yaw or pitch angles up to 3^o (Figures 17 and 18).

4. The measured pressure distributions are unaffected by changes in velocity or static pressure (Figure 23).

5. The existing location of the pressure intake for the immersion gear gives a pressure lower than hydrostatic and causes the torpedo to ride below set depth.

6. True hydrostatic pressure, independent of velocity and small yaw or pitch angles, will be obtained if the immersion gear hydrostat is connected to points midway between the tail fins and about 23" ahead of the tip of the tail.

7. The depth and roll recorder is so located in the exercise head that it is subject to a pressure lower than true hydrostatic and too shallow a depth is recorded. Unfortunately, it is possible for the recorder to indicate the depth to be the set depth when the torpedo rides low, as described in Item 5 above.

8. Since there is no satisfactory location in the exercise head where a pressure connection will give $P = P_0$, it is recommended that the included pressure data be used to estimate corrections for application to the recorder in its existing location.

9. Form drag and moment coefficients calculated from pressure distribution data are about 15% higher than given by Water Tunnel measurements while the calculated cross force is 27% lower than measured.

10. The K values for the inception of cavitation on the projectile nose as obtained by actual observation and by prediction from the pressure measurements are in good agreement.

It should be noted that these tests were made with the standard fin tail without a shroud ring and some of the above conclusions (particularly Item 6), cannot be expected to apply when the ring is added. Additional measurements with a ring tail are being made.

PRESSURE DISTRIBUTION MEASUREMENTS ON THE MK 13-1, 13-2, AND 13-2A TORPEDOES

I. PURPOSE AND SCOPE OF INVESTIGATION

This report is the fourth in a series covering Water Tunnel tests on the U. S. Navy Torpedo Mk 13, Modifications 1, 2, and 2A. The first of these was a basic investigation of the hydrodynamic characteristics of these torpedoes.[1] The second report [2] dealt with the possible improvement in the stability and control of the torpedoes by the addition of a shroud ring tail. The third covered Water Tunnel tests of these torpedoes with crown and spade noses [3]. The tests reported herein were made to investigate the pressure distribution about the bodies of these torpedoes, and the effect on the pressure distribution of variations in velocity, static pressure (submergence), and orientation with respect to the line of travel. These tests, as well as those covered by the preceding reports, were made on 2" diameter models in the High Speed Water Tunnel at the California Institute of Technology [4]. The tests were authorized by Dr. E. H. Colpitts, Chief of Section 6.1, NDRC, in a letter dated April 16, 1943.

The main objective of this investigation was to determine whether the present location of the pressure inlet to the hydrostat of the immersion (depth control) mechanism is contributing to the erratic behavior of these torpedoes with respect to depth keeping, and, if so, to suggest the means for overcoming this difficulty. The pressure distribution data obtained from these tests are also useful for determining whether the depth and roll recorder indicates actual running depth, for checking the cavitation characteristics of the torpedo, and may be used to calculate the cross force, moment, and form drag acting on the torpedo within the range of velocities and yaw angles covered by these tests.

The tests made included measurements of the pressure distribution about the body with and without fins, under conditions of constant velocity and constant static pressure (i.e., constant submergence), and with varying yaw between -6 and +6 degrees. Additional tests were made to determine the effect, if any, of variations in static pressure and velocity on the pressure distribution.

II. APPARATUS AND TEST PROCEDURES

Model Construction

The stainless steel model used in these tests is shown in Figures 1 to 3, and has a maximum diameter of 2" and an overall length of 14.37" (model scale 1:11.21). Since all three prototype torpedoes are exactly alike in external shape and dimensions, they may all be represented by a single model. The model consists of

(1) Numbers in parentheses refer to references in Appendix D

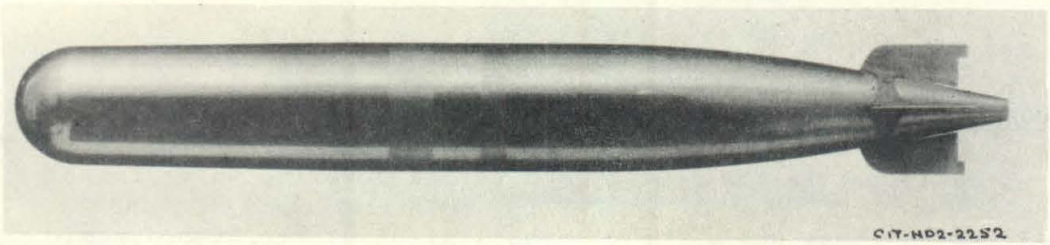

FIGURE 1

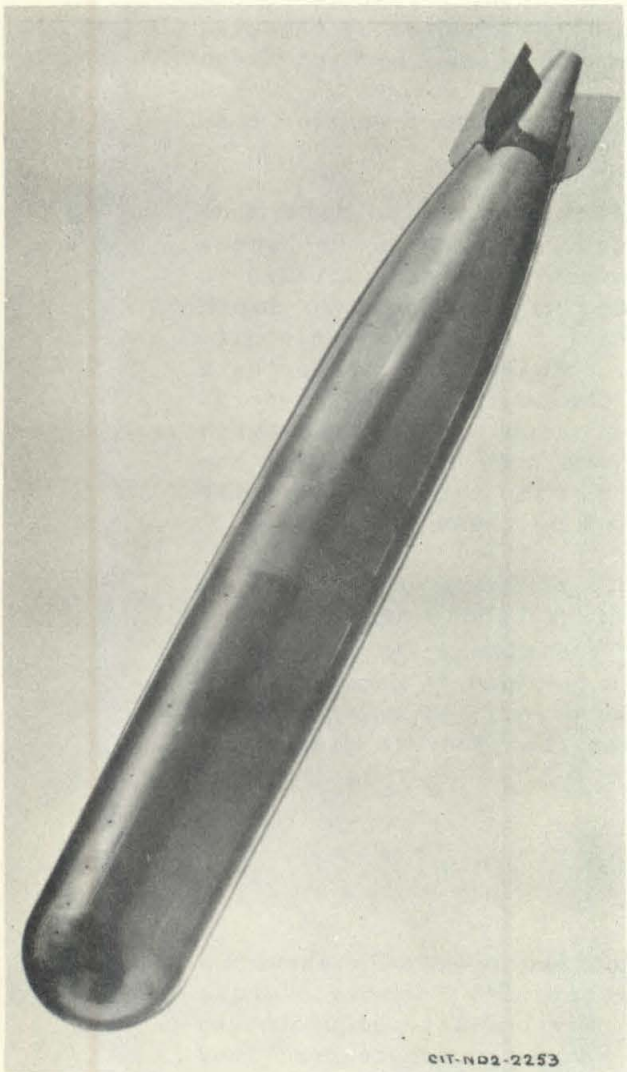

FIGURE 2

MODEL WITH FINS

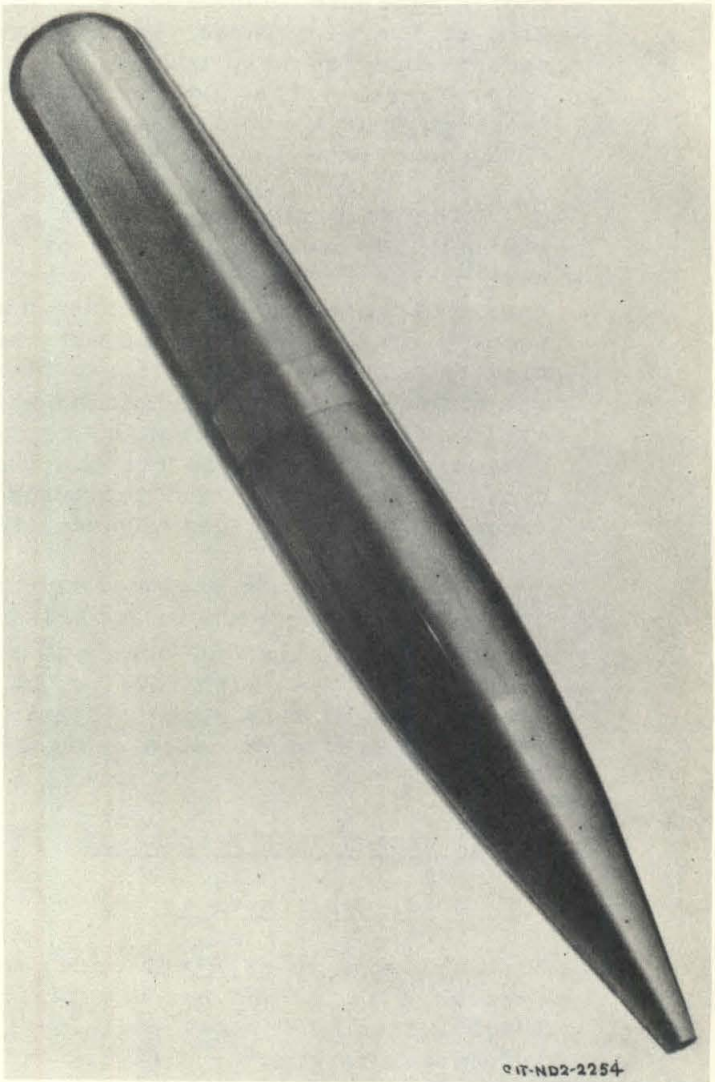

FIGURE 3

FINLESS MODEL

NOTE PIEZOMETER OPENINGS IN TWO LOWER VIEWS

a hollow forebody, a hollow afterbody, and a separate tail cone, all supported by the spindle-mounted center section. Two interchangeable tail cones were provided, one finless and one with fins and with rudders fixed in neutral position. The forebody, afterbody, and tail cones were so made that each part could be rotated about the longitudinal axis independently of the other parts. With this arrangement, a single row of piezometer openings distributed along a meridian is sufficient for exploring the pressure distribution about the entire body. To avoid crowding the seven piezometer taps on the nose, three of them were located on a line at right angles to the main row of taps (see Figure 2). A protractor scale scribed at the joint line of each body section and graduated in 5 degree intervals provided the means for setting the angular position of the piezometer taps.

Piezometer Openings and Pressure Leads

The piezometer openings were made by drilling 1/16" holes at right angles to the surface before making the final finishing cut on the outside. Each hole was then plugged with a stainless steel rod extending about 3/16" into the body. A nickel-silver tube of 1/16" OD and 1/32" ID was inserted in the hole from the inside and silver-soldered in place. A finishing cut was then taken over the entire surface and a 1/32" diameter hole was then drilled through each plug and reamed, thus leaving the piezometer openings flush with the surface and normal to it and with sharp square corners. Twenty such openings were provided on the finless model and 19 on the model with fins. The location of these holes is shown in Figure 6.

Rubber tubes were used to connect these nickel-silver tubes to a bundle of similar tubes which extended from the outside of the Water Tunnel, through the model supporting strut, and into the model through an opening in the bottom of the center section, as shown in Figures 4 and 5. The slenderness of the strut limited the number of tubes that could be carried through it to 12. It was necessary, therefore, to measure the pressure distribution about the forebody and about the afterbody in separate test runs. Outside the tunnel working section, each tube terminated in a valve mounted on a common manifold, so that each piezometer tap could, in turn, be connected to the differential pressure gage.

Differential Pressure Gage

The differential pressure gage used in these tests consists of a flat-tube helical element inside a pressure-tight case. One end of the helix is attached to the case and the other end, which is free to turn, is attached to a swinging mirror mounted on flexible hinges. A ray of light from a straight-filament bulb enters the case through a round window in front of the mirror and is reflected by the swinging mirror onto a curved scale. The window glass is a lens which focuses an image of the straight-wire filament upon the curved scale. To measure a pressure differential, the high-pressure side is connected to the helical element and the

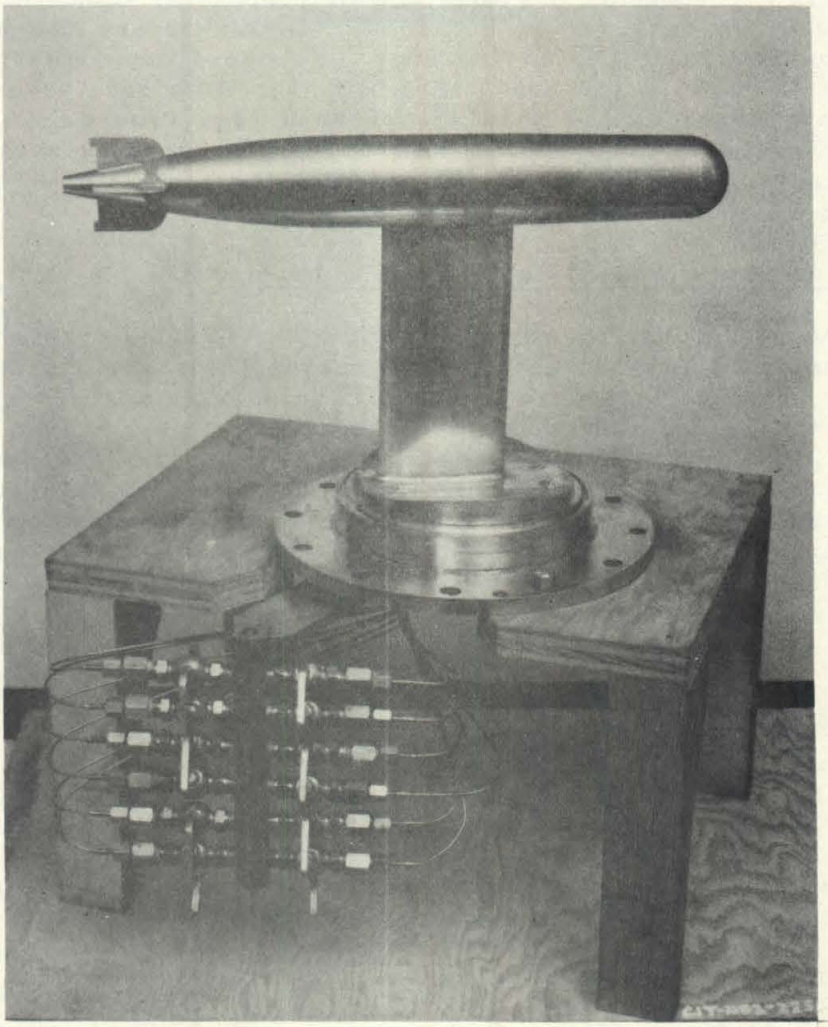

FIGURE 4

MODEL ASSEMBLED ON STREAMLINED STRUT
WITH BASE PLATE AND TUBE MANIFOLD,
READY FOR INSTALLATION IN THE TUNNEL

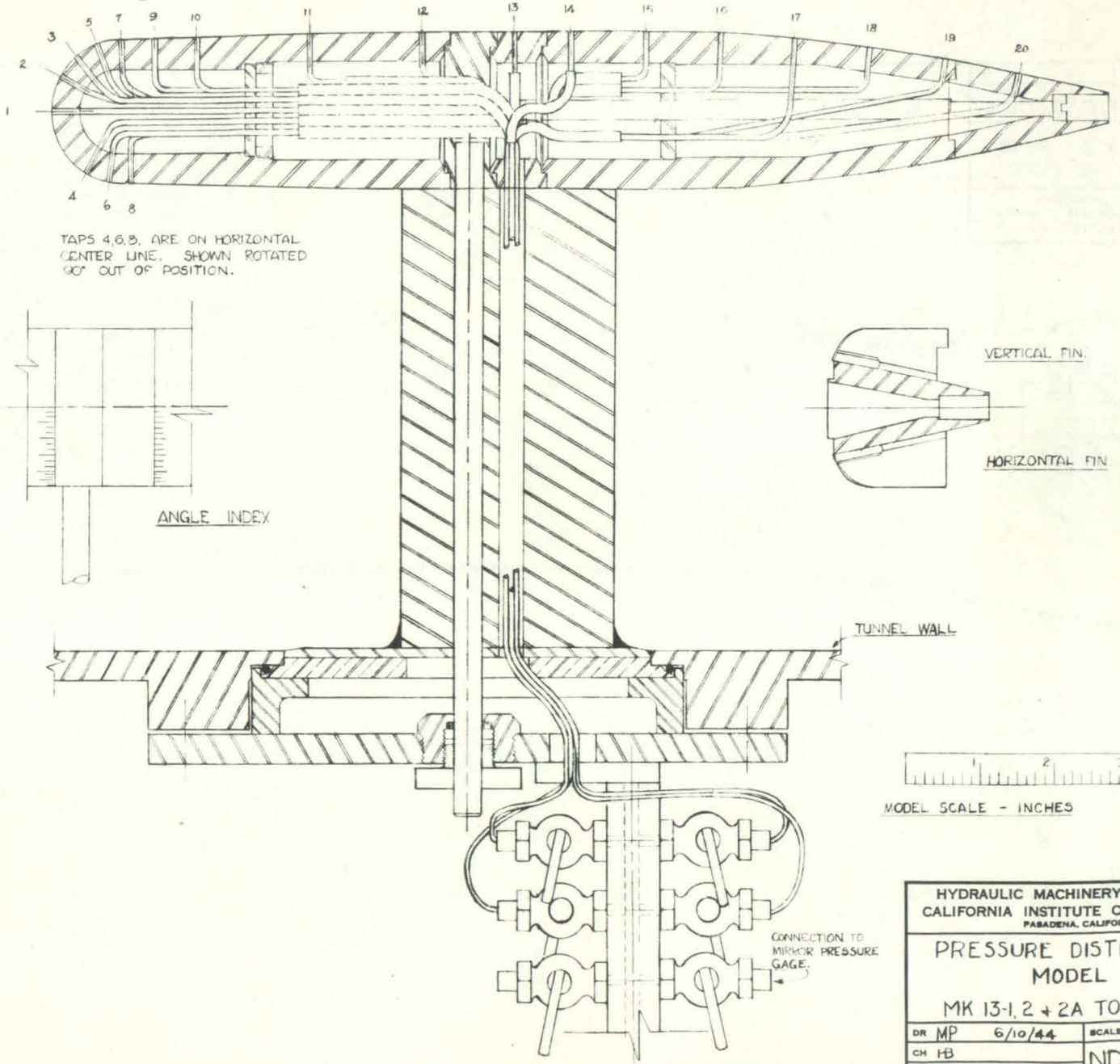

HYDRAULIC MACHINERY LABORATORY
CALIFORNIA INSTITUTE OF TECHNOLOGY
PASADENA, CALIFORNIA

PRESSURE DISTRIBUTION MODEL

MK 13-1, 2 + 2A TORPEDOES

DR MP 6/10/44	SCALE FULL
CH HB	ND-871 -Z
AP	

FIGURE 5

CONFIDENTIAL

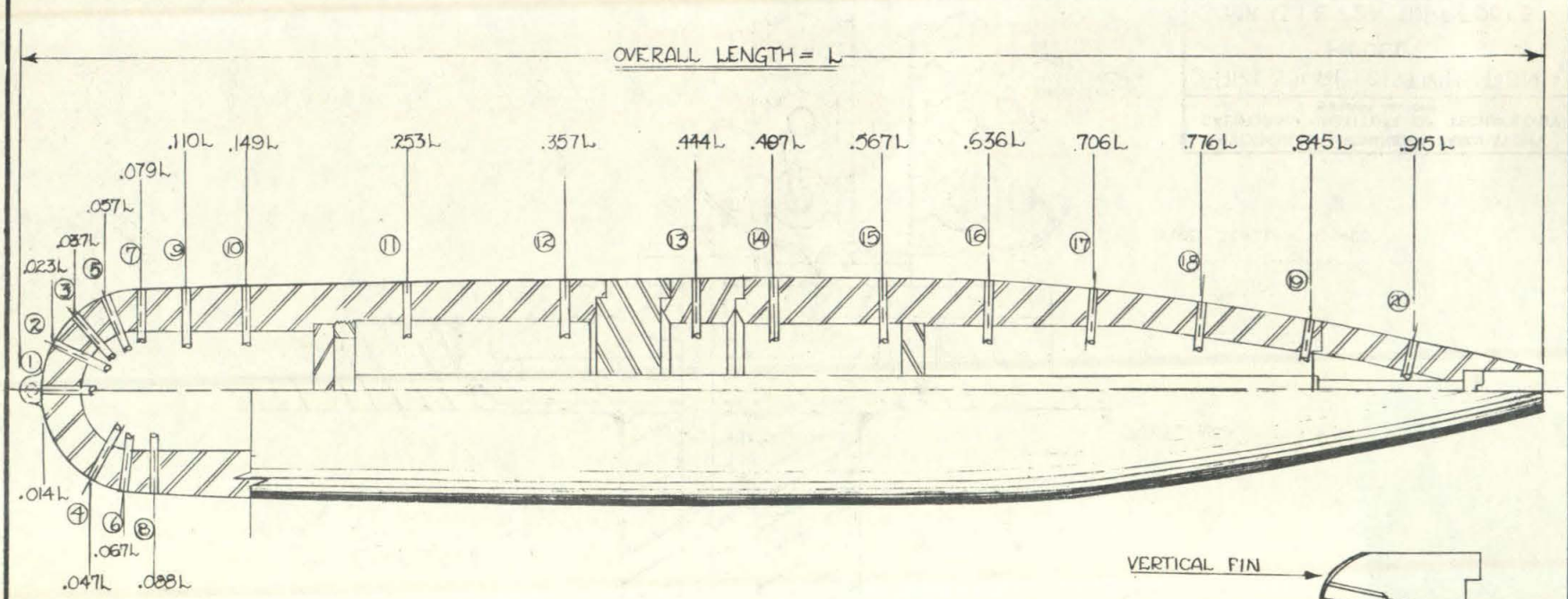

TAPS 4,6,8, ARE ON HORIZONTAL CENTER LINE. SHOWN ROTATED 90° OUT OF POSITION.

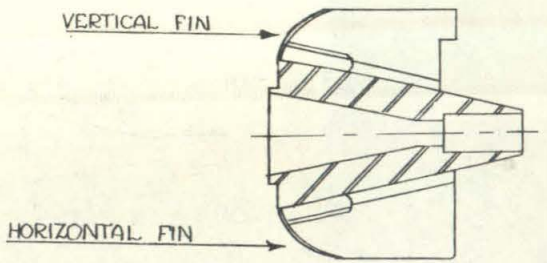

ANGULAR LOCATION OF NOSE TAPS

TAP NO.	ANGLE FROM AXIS
1	0°
2	30°
3	50°
4	60°
5	70°
6	80°

HYDRAULIC MACHINERY LABORATORY
CALIFORNIA INSTITUTE OF TECHNOLOGY
PASADENA, CALIFORNIA

PRESSURE TAP LOCATION
MK. 13-1, 2, & 2A TORPEDOES

DR MP 6/13/44	SCALE FULL
CH HB	ND-870-U
AP	

FIGURE 6

low-pressure side to the case. The scale of the gage is 50 cm long, and a full-scale deflection is equivalent to 11 pounds per square inch.

Test Procedure

The pressure distribution around the torpedo was explored by setting the piezometer taps at a given angle with the vertical centerline and measuring the pressure at each tap for yaw angles from -6 to +6 degrees in one degree intervals. The piezometer tap settings were varied from 0 to 90° in 15° steps. Because of the symmetry of the torpedo, these measurements give the pressure distribution about the entire body. Most of the tests were made with constant velocity of 32.8 feet per second and constant static pressure in the tunnel working section of 10 psi. Several test runs were made with different velocities and static pressures to determine the effect of these variables on the pressure distribution.

III. TEST RESULTS

The test results are shown in Figures 7 to 23, inclusive, and are presented in terms of p/q, where

$p = P - P_o$

P = pressure on the surface of the torpedo, pounds per square foot

P_o = static pressure in undisturbed water at same level as torpedo centerline, pounds per square foot

$q = 1/2\ \rho\ V^2$ = dynamic pressure of water, pounds per square foot

ρ = mass density of water, slugs per cubic foot

V = mean water velocity, feet per second

The static pressure reference was taken at the tunnel wall at a point 5.25 model diameters upstream of the nose. The differential pressure measured at each piezometer opening was corrected for tunnel pressure gradient by subtracting from it the tunnel pressure drop, measured in the absence of the model, between the reference point and a point opposite that piezometer opening.

To reduce the bulk of the data presented herein, the curves show the pressure distribution for yaw angles of 0, 3, and 6 degrees only, although measurements were made at one degree intervals.

Longitudinal Pressure Distribution - Zero Yaw

In Figure 7 is shown the longitudinal pressure distribution around the finless torpedo at zero yaw, plotted against distance

from the tip of the towing ring divided by overall length. Pressure measurements were made with the piezometer taps rotated between zero and 90° from the vertical in 15° steps. It is evident that, for a symmetrical body oriented with its axis parallel to the direction of motion, the pressure around any section normal to the axis should be constant. It is seen that except for the points on the nose, where the pressure changes very rapidly, the test points do not deviate much from the mean value. The maximum deviation for any point aft of the nose hemisphere is ±2.5% of the dynamic pressure.

From full stagnation pressure at the tip of the nose, the pressure drops very rapidly to about 0.78 q below static and then rises again, but remains below static pressure over almost the entire length of the torpedo. The pressure on the body equals the static pressure ($P = P_0$) at two stations, one on the projectile nose and one on the afterbody.

It will be noted that only one test point is shown for tap No. 13 (at 0.445 L). This tap is located in the center-section of the model, which cannot be rotated. This tap, therefore, measures the pressure on the vertical center line only. Figure 8 shows the longitudinal pressure distribution around the torpedo with fins at zero yaw. Comparing this figure with Figure 7, it is seen that the presence or absence of the fins does not affect the pressure on the forward 60% of the torpedo length. The presence of the fins causes a larger pressure drop on the forward portion of the afterbody taper and a steeper pressure rise toward the tail. It will be noted also, that on piezometer tap No. 19, the pressure is higher when immediately in front of a fin (0° and 90° positions) than it is for all positions between the fins.

Yaw Effects on Longitudinal Pressure Distribution

Figures 9 and 10 show the longitudinal pressure distribution on the body without and with fins, respectively, as affected by yaw or pitch. These curves show the pressure along a longitudinal section at right angles to the plane of yaw or pitch. From a consideration of the symmetry of the body, it is evident that the pressure distribution along the top and bottom meridians when the torpedo yaws to either starboard or port, is exactly the same as the pressure distribution along the sides (on the horizontal meridians) of the torpedo as it pitches up or down. It is seen that the effect of yaw or pitch is to lower the pressure over the entire length, very slightly for angles below 3°, and more noticeably for larger angles.

In Figures 11 and 12 is shown the longitudinal pressure distribution on the windward and leeward side, respectively, of the finless hull along the meridians at 45° with the planes of yaw or pitch. It is seen that yaw causes the pressure on the nose to increase on the windward side and to decrease on the lee side. Along the mid-portion of the hull, the pressure on both sides decreases with yaw, and near the tail the pressure decreases with

yaw or pitch on the windward side and increases slightly on the lee side.

Figures 13 and 14 give the same data for the hull with fins as shown in the preceding two figures for the finless hull. A comparison of the curves of these figures with those of Figures 11 and 12, shows that the presence of the fins does not materially affect the pressure on the 45 degree planes.

Figures 15 and 16 show the longitudinal pressure distribution along the windward and lee sides, respectively, of the finless hull along a section in the plane of yaw or pitch, i.e., along the sides if yawing, and along top and bottom when pitching. Figures 17 and 18 give the same information about the hull with fins. It is seen that, in general, the effect of yaw on the pressure distribution on these planes is about the same as in the 45 degree planes, except that the pressure on the afterbody with fins is less affected by yaw or pitch.

Pressures Around Cross Sections Normal to Torpedo Axis

In Figures 19 to 22, inclusive, are presented the transverse pressure distributions around cross sections taken normal to the axis of the torpedo at each piezometer opening or station. The curves show the pressures for yaw angles of 0, 3, and 6 degrees, plotted against body angles measured to either side from the vertical centerline. Again, from symmetry considerations, it is evident that these curves give also the pressure distribution when the torpedo is pitching, if we measure the body angles from the horizontal centerline instead of the vertical. Also, the body angles may be reckoned from either end of the centerline (i.e., either from top or bottom, or from port side or starboard side) since the pressure distribution is symmetrical about the 90 degree points on windward and lee sides. Figures 19 and 20 cover the stations on the forebody. Since the presence or absence of the fins does not affect the pressure on the forebody, these curves apply to the torpedo with fins as well as to the finless hull. Figure 21 gives the pressure distribution on the finless afterbody and Figure 22 on the afterbody with fins. A comparison of these last two figures again shows how the fins cause slightly lower minimum pressures on the forward part of the afterbody (Stations 16 and 17) and how they cause higher pressures further aft in the immediate vicinity of each fin (Station 19).

It will be noted that Stations 1 and 13 are not shown on these curves. Station 1 is at the tip of the nose and Station 13 is on the fixed center section of the model. Neither one of these piezometers, therefore, is capable of measuring the pressure around a normal section.

Effect of Velocity and Static Pressure

The curves shown in Figure 23 were taken at two different static pressures (10 and 20 psi) and with velocities varying from 25.8 to 56.4 fps. These curves show that the pressure distribution is independent of both the static pressure and the velocity.

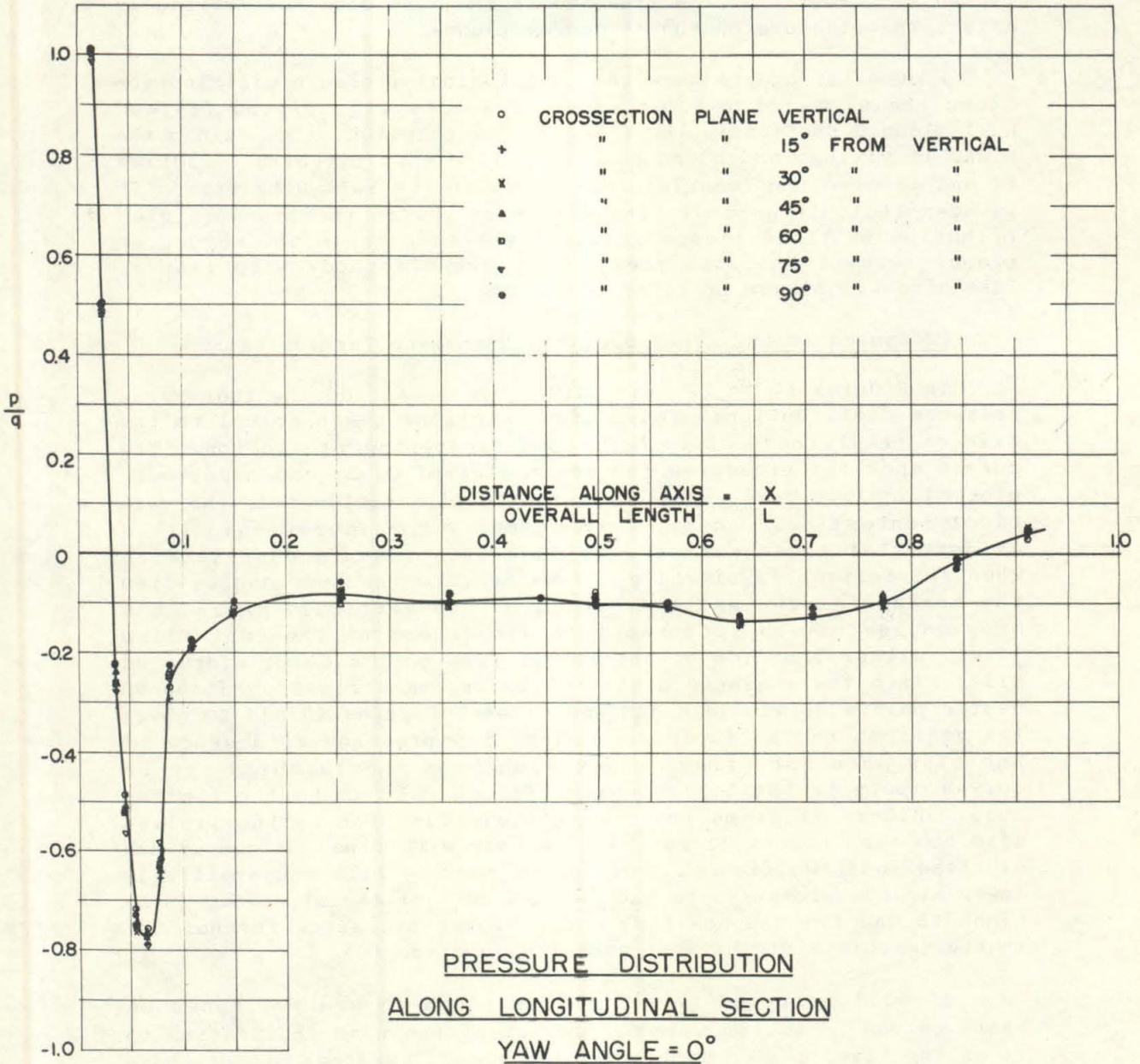

PRESSURE DISTRIBUTION

ALONG LONGITUDINAL SECTION

YAW ANGLE = 0°

BODY WITHOUT FINS

CIT — HML
ND 15-3163 M

FIGURE 7

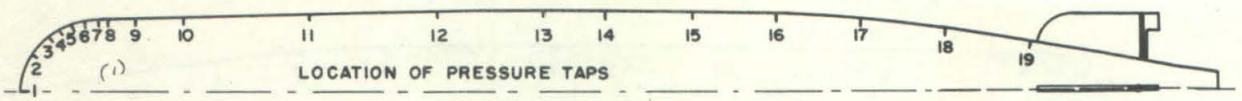

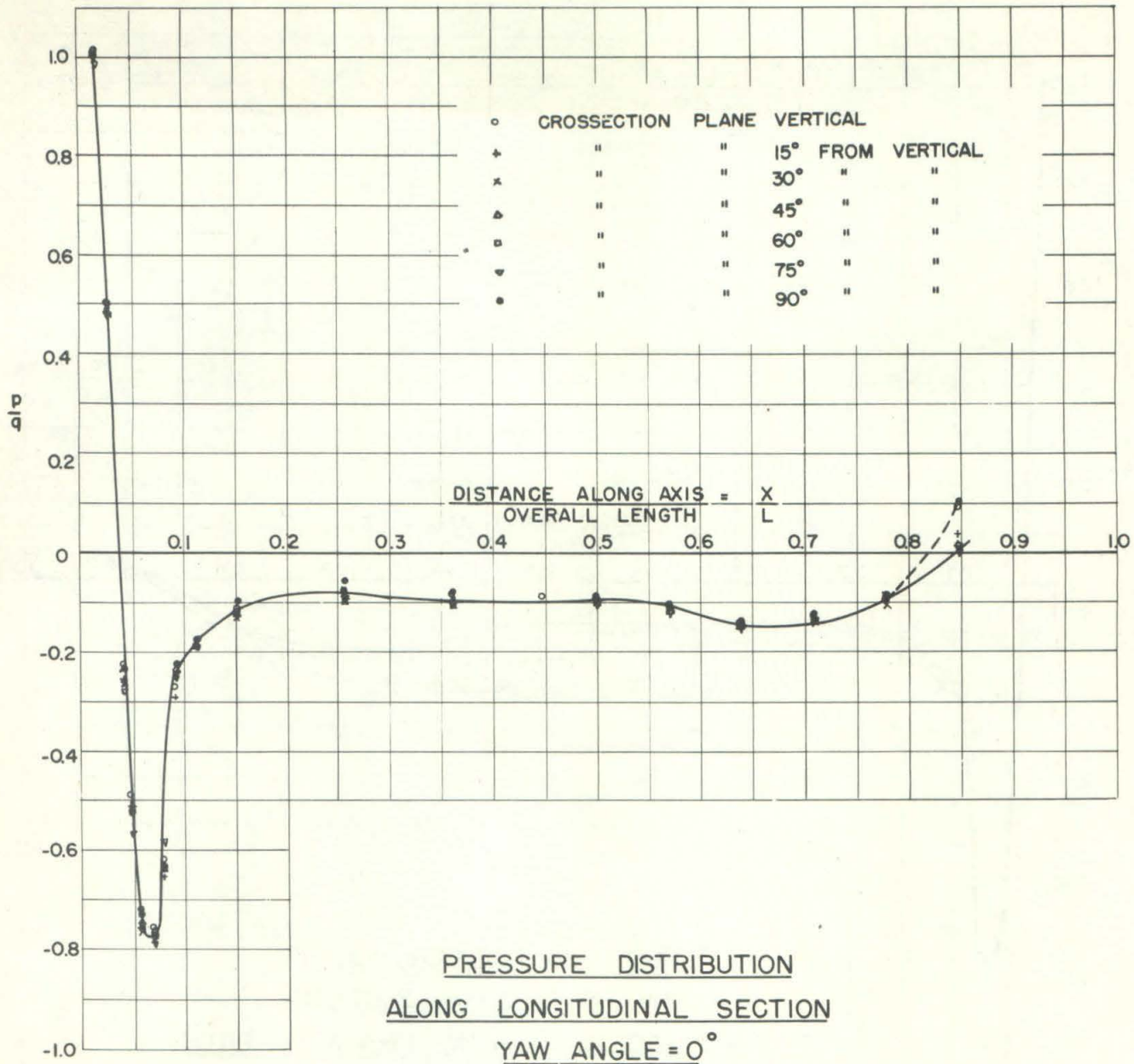

PRESSURE DISTRIBUTION

ALONG LONGITUDINAL SECTION

YAW ANGLE = 0°

BODY WITH FINS

CIT – HML
ND 15 - 3164 M

FIGURE 8

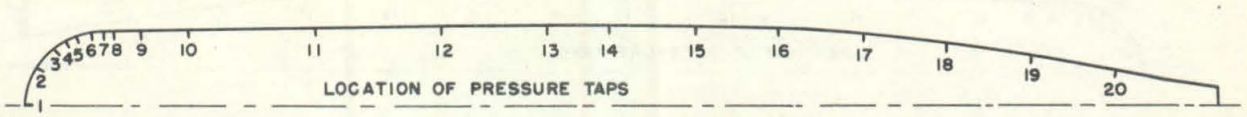

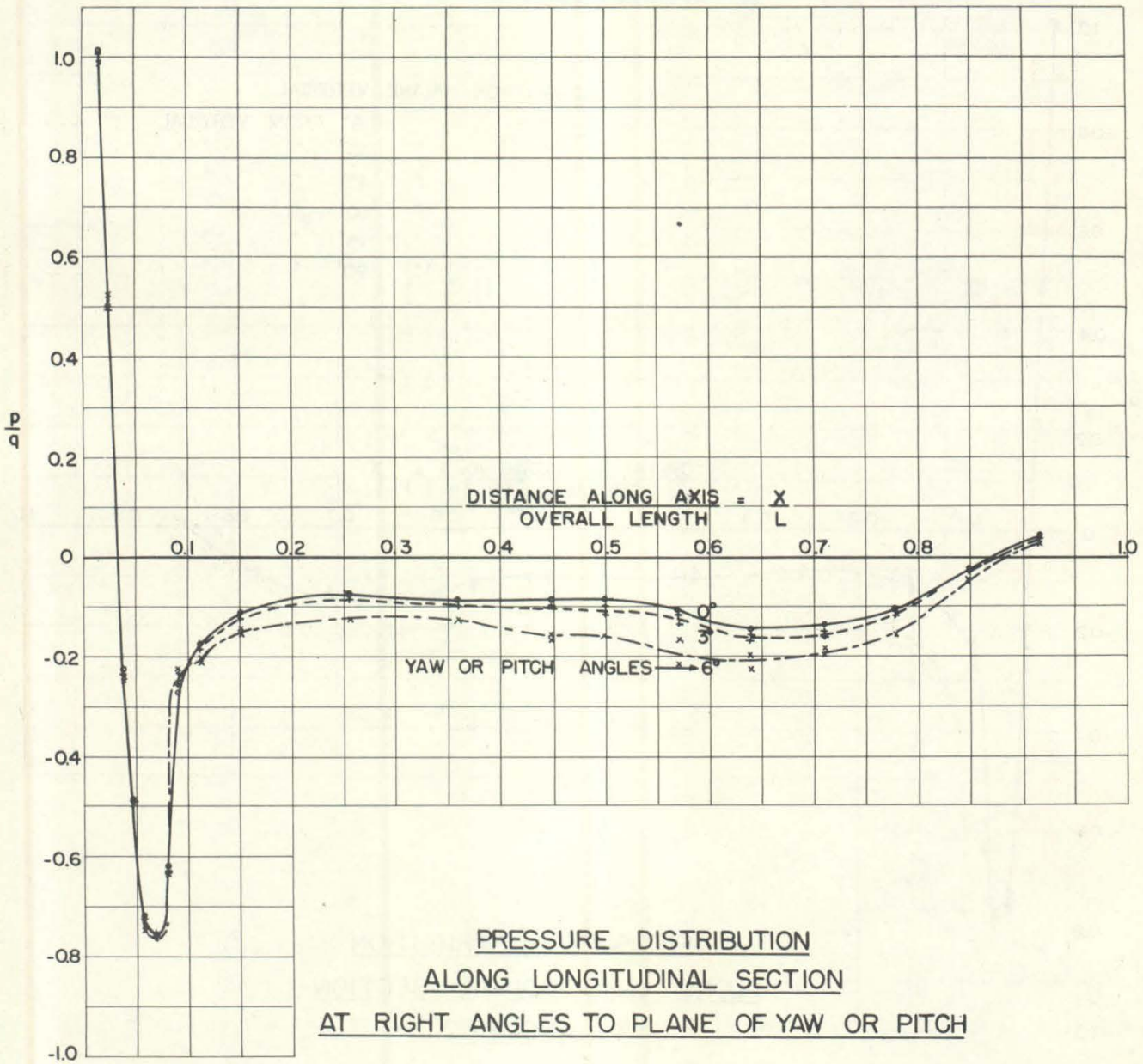

PRESSURE DISTRIBUTION
ALONG LONGITUDINAL SECTION
AT RIGHT ANGLES TO PLANE OF YAW OR PITCH

BODY WITHOUT FINS

CIT — HML
ND 15 - 3165 M

FIGURE 9

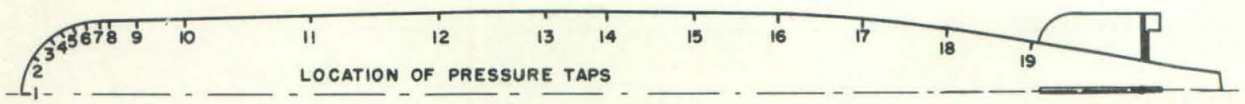

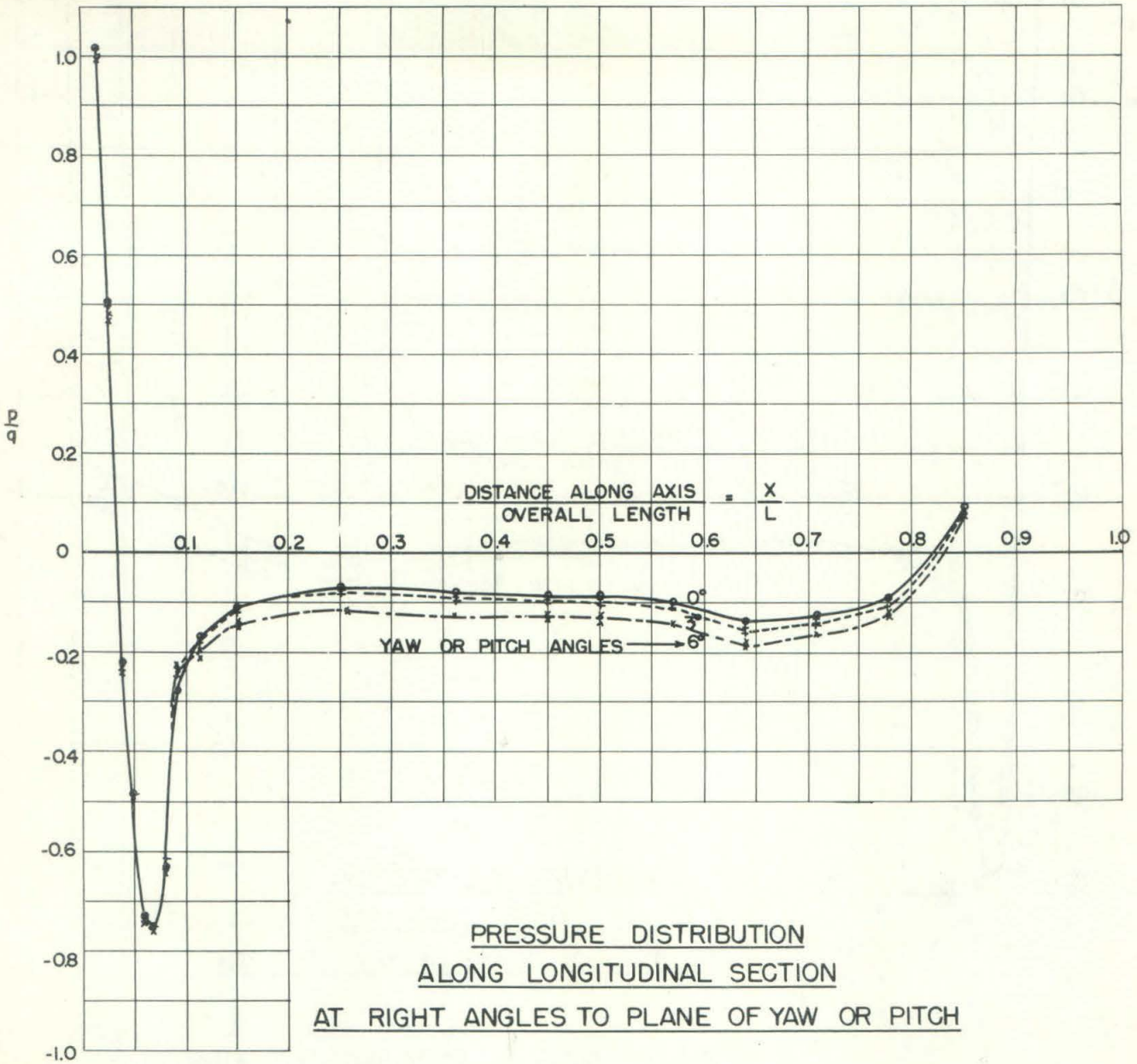

PRESSURE DISTRIBUTION
ALONG LONGITUDINAL SECTION
AT RIGHT ANGLES TO PLANE OF YAW OR PITCH

BODY WITH FINS

CIT – HML
ND 15-3166 M

FIGURE 10

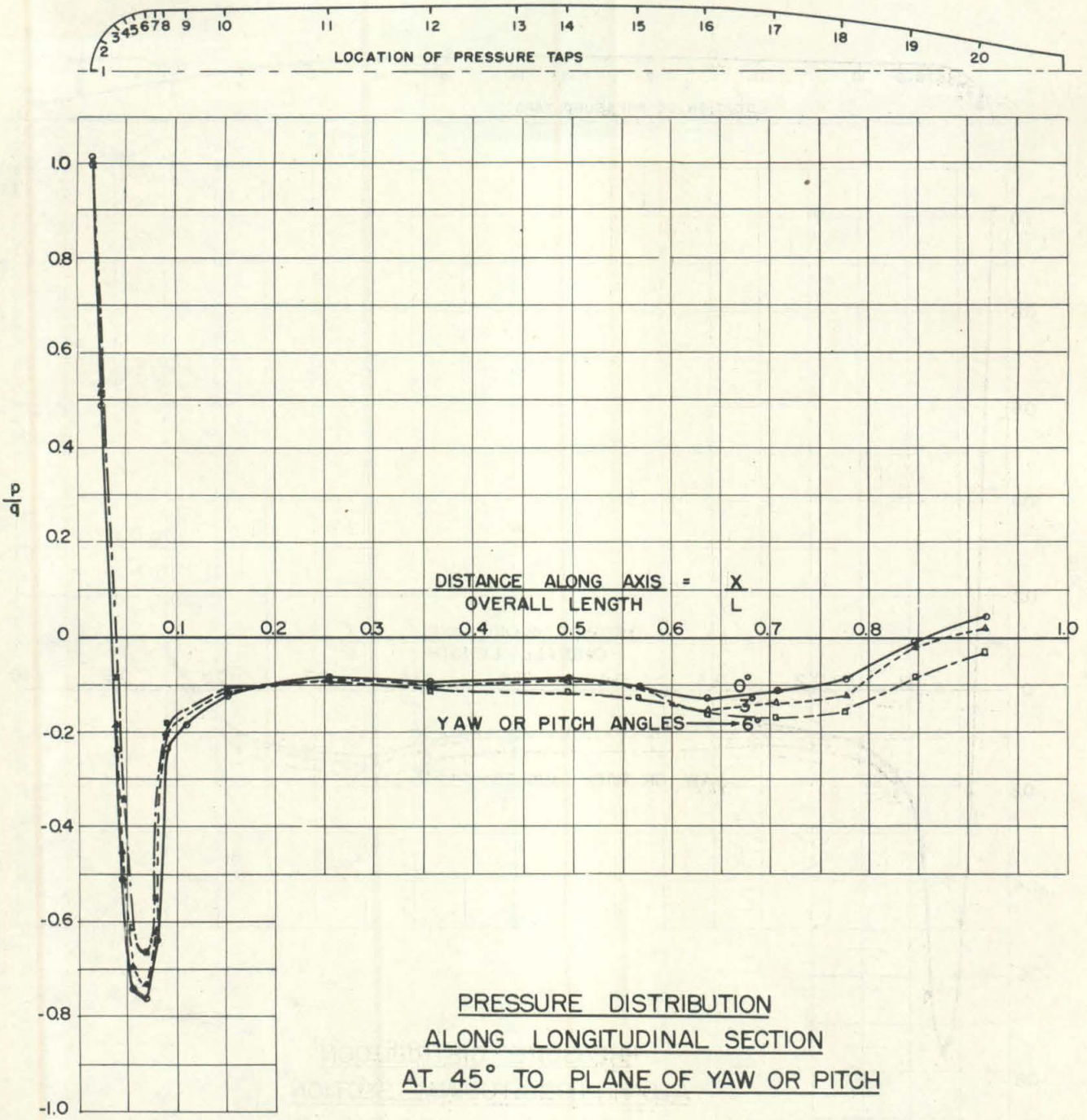

PRESSURE DISTRIBUTION
ALONG LONGITUDINAL SECTION
AT 45° TO PLANE OF YAW OR PITCH

WINDWARD SIDE OF BODY WITHOUT FINS

CIT – HML
ND 15-3167 M

FIGURE 11

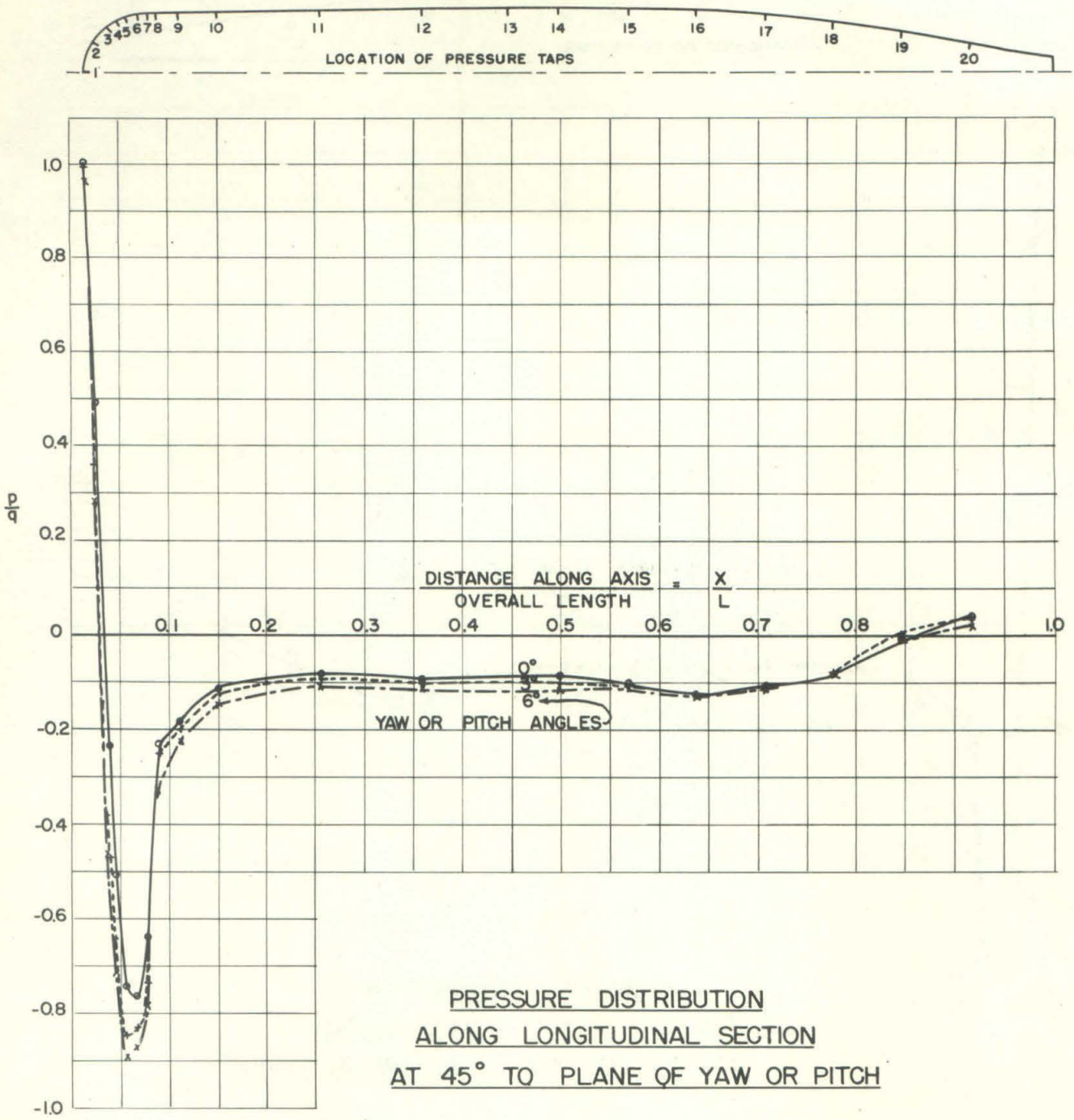

PRESSURE DISTRIBUTION
ALONG LONGITUDINAL SECTION
AT 45° TO PLANE OF YAW OR PITCH

LEE SIDE OF BODY WITHOUT FINS

CIT – HML
ND 15 - 3168 M

FIGURE 12

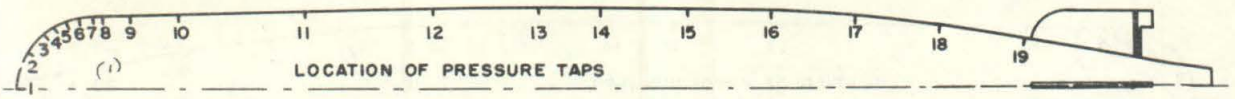

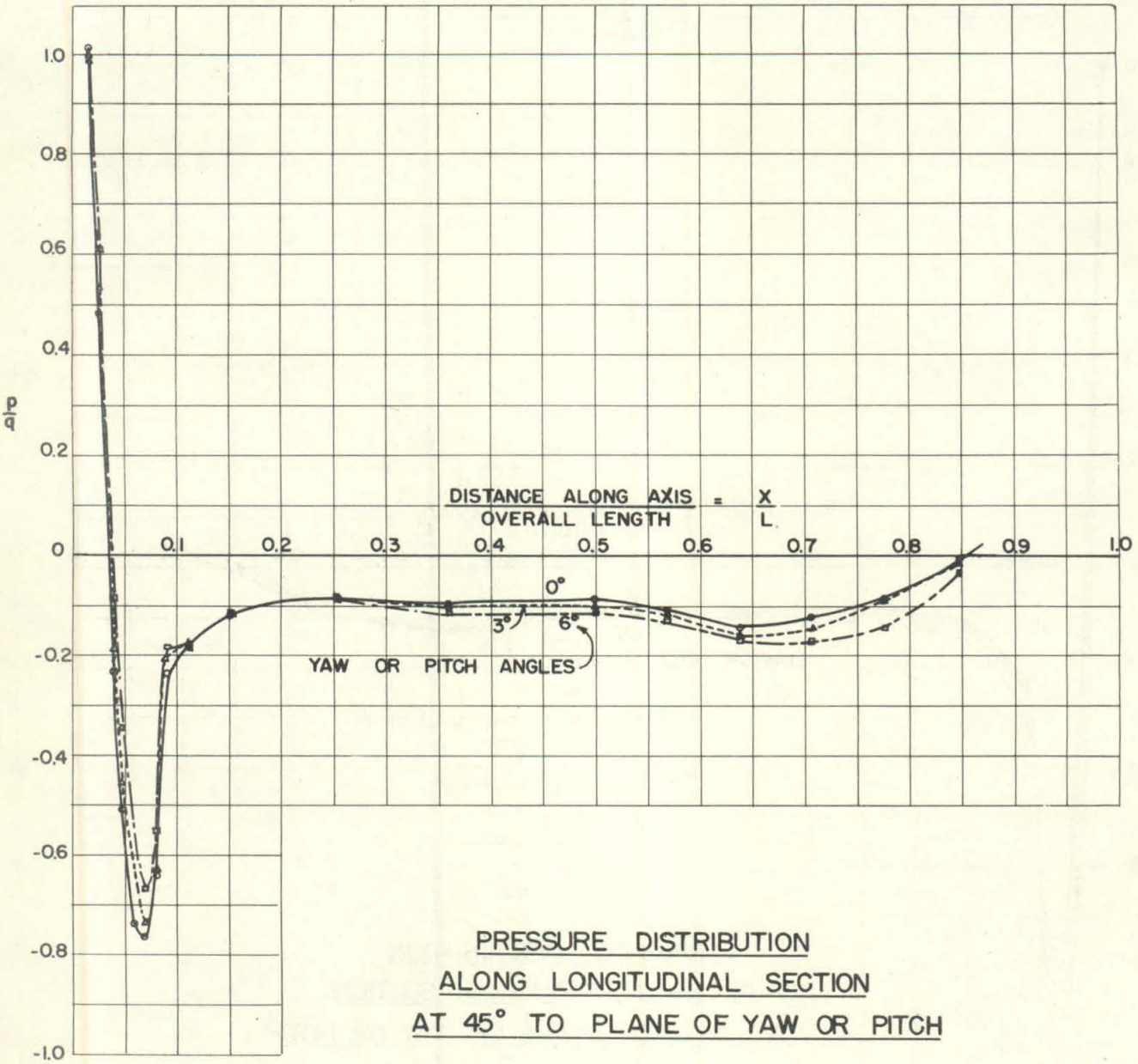

PRESSURE DISTRIBUTION
ALONG LONGITUDINAL SECTION
AT 45° TO PLANE OF YAW OR PITCH

WINDWARD SIDE OF BODY WITH FINS

CIT – HML
ND 15-3169 M

FIGURE 13

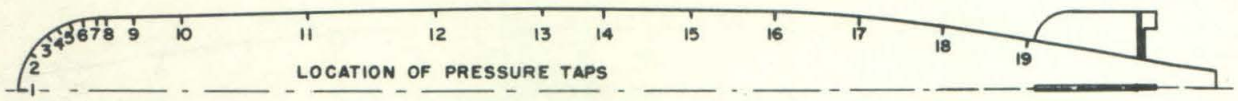

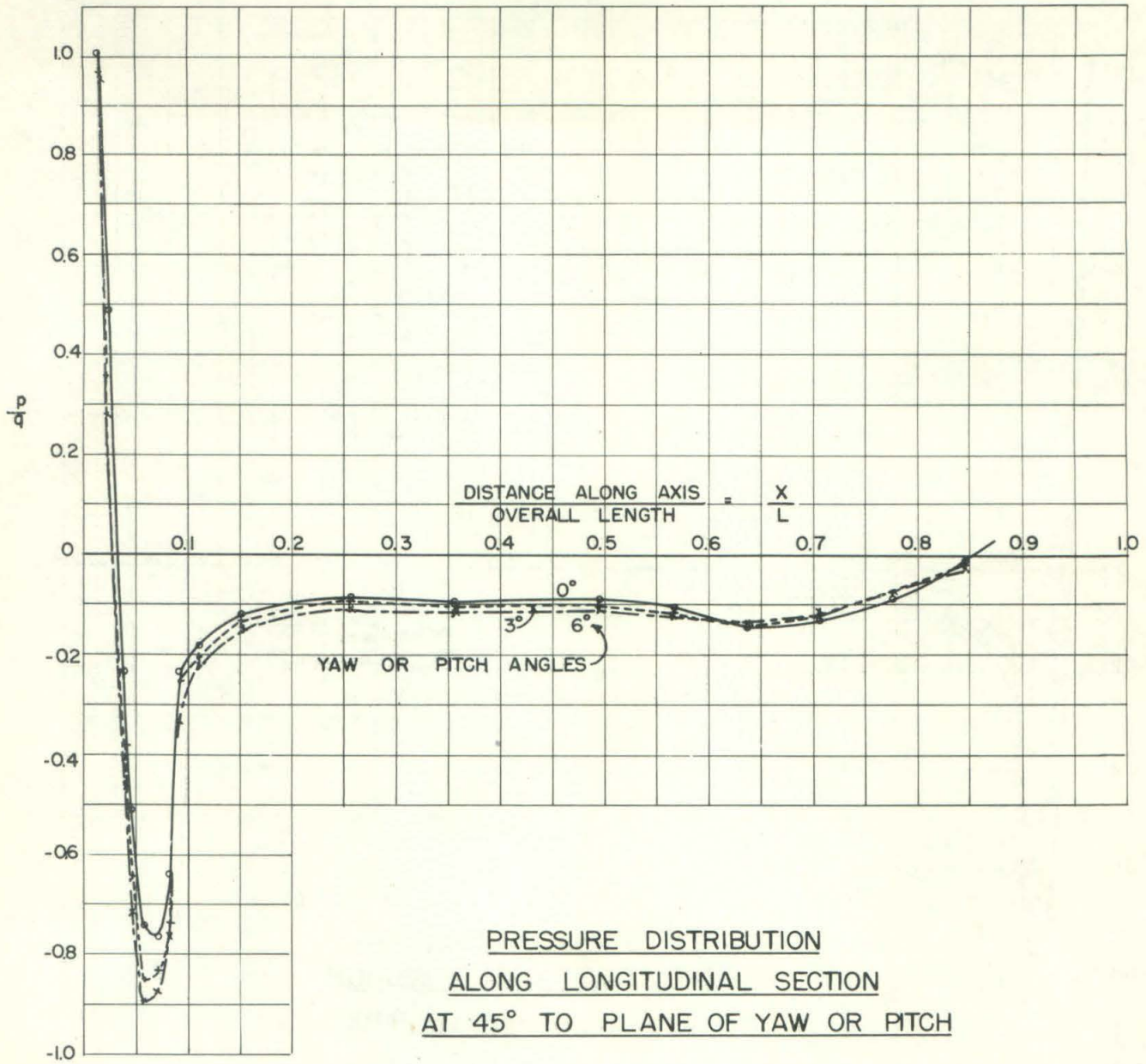

PRESSURE DISTRIBUTION
ALONG LONGITUDINAL SECTION
AT 45° TO PLANE OF YAW OR PITCH

LEE SIDE OF BODY WITH FINS

CIT — HML
ND 15-3170 M

FIGURE 14

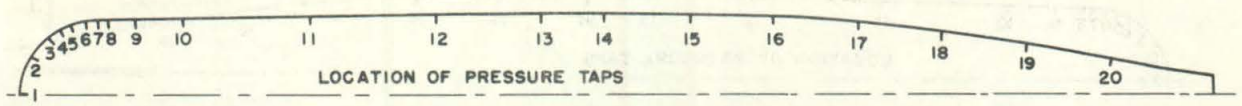

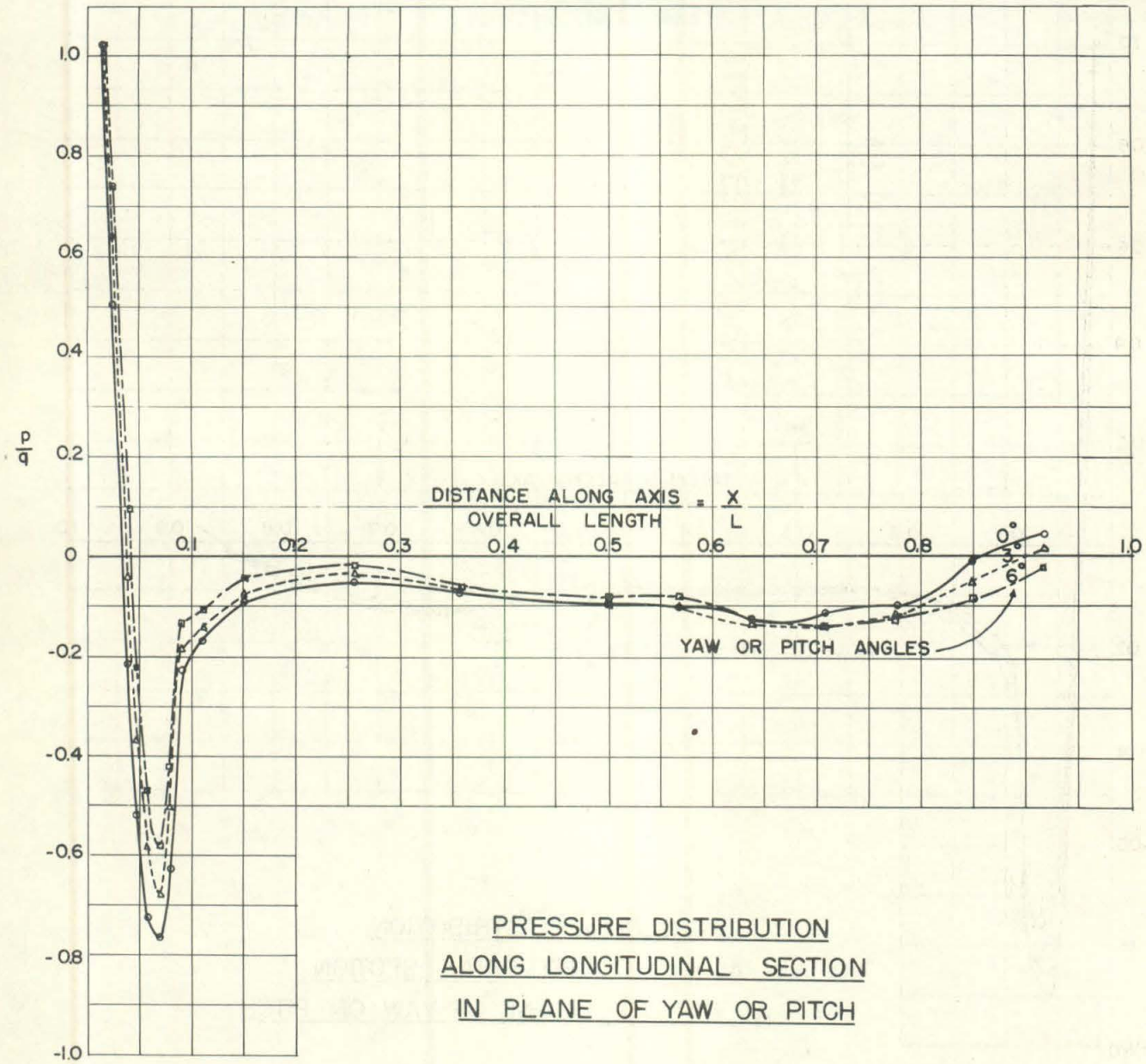

PRESSURE DISTRIBUTION
ALONG LONGITUDINAL SECTION
IN PLANE OF YAW OR PITCH

WINDWARD SIDE OF BODY WITHOUT FINS

CIT — HML
ND 15-3171 M

FIGURE 15

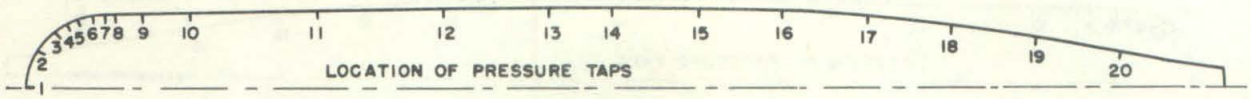

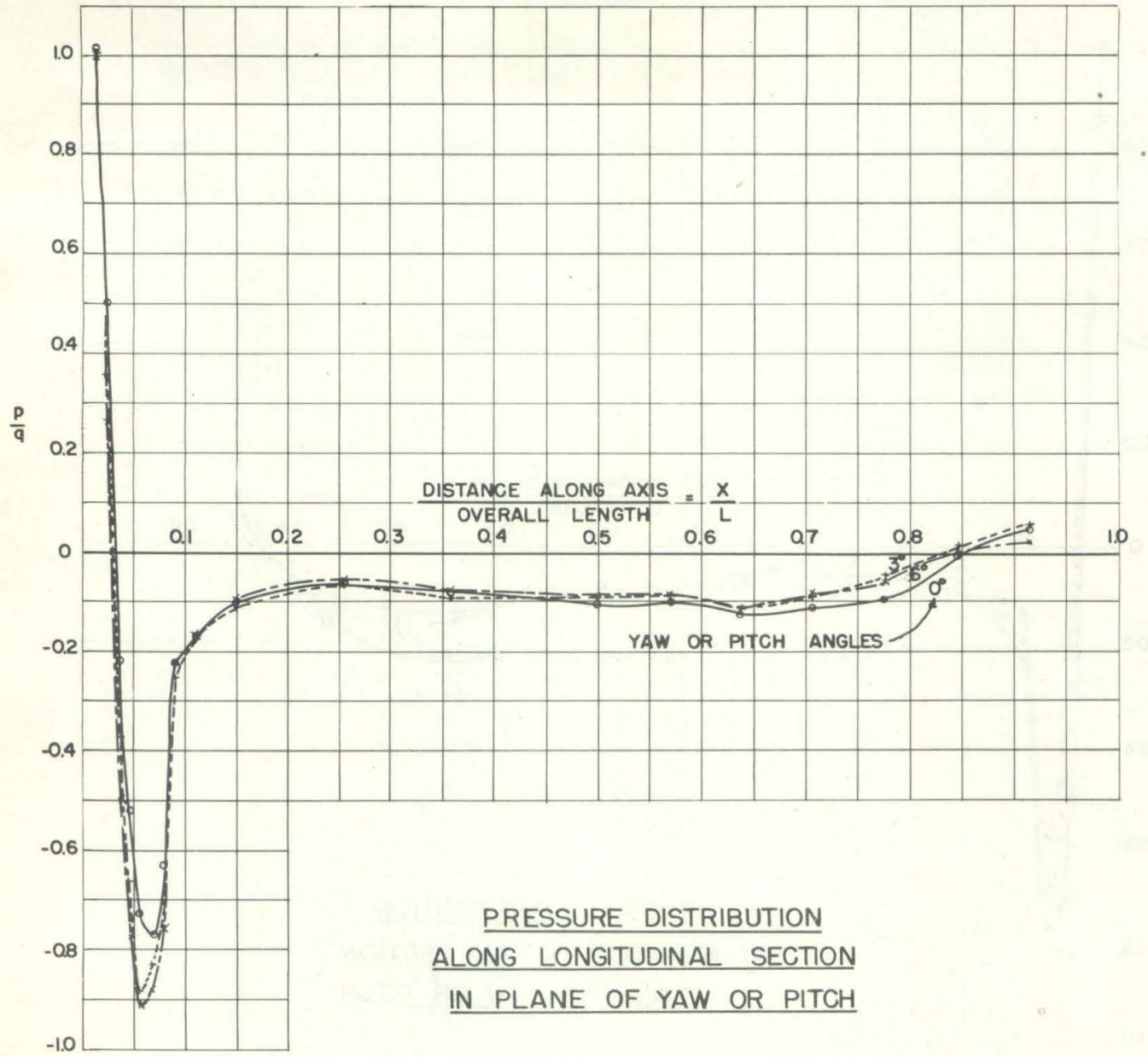

PRESSURE DISTRIBUTION
ALONG LONGITUDINAL SECTION
IN PLANE OF YAW OR PITCH

LEE SIDE OF BODY WITHOUT FINS

CIT — HML
ND 15-3172 M

FIGURE 16

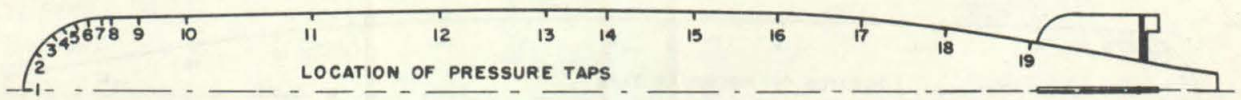

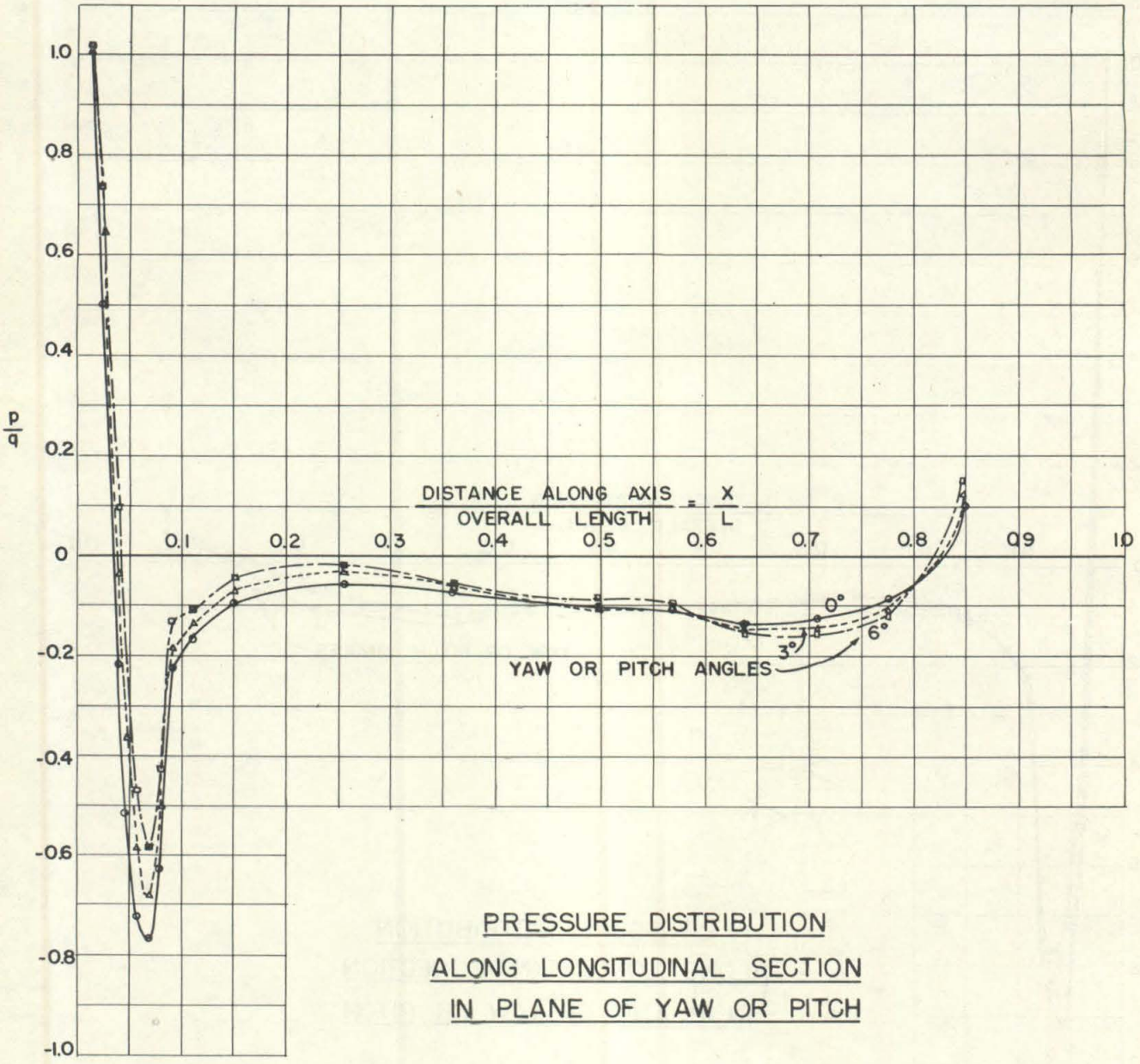

PRESSURE DISTRIBUTION
ALONG LONGITUDINAL SECTION
IN PLANE OF YAW OR PITCH

WINDWARD SIDE OF BODY WITH FINS

CIT — HML
ND 15 - 3173 M

FIGURE 17

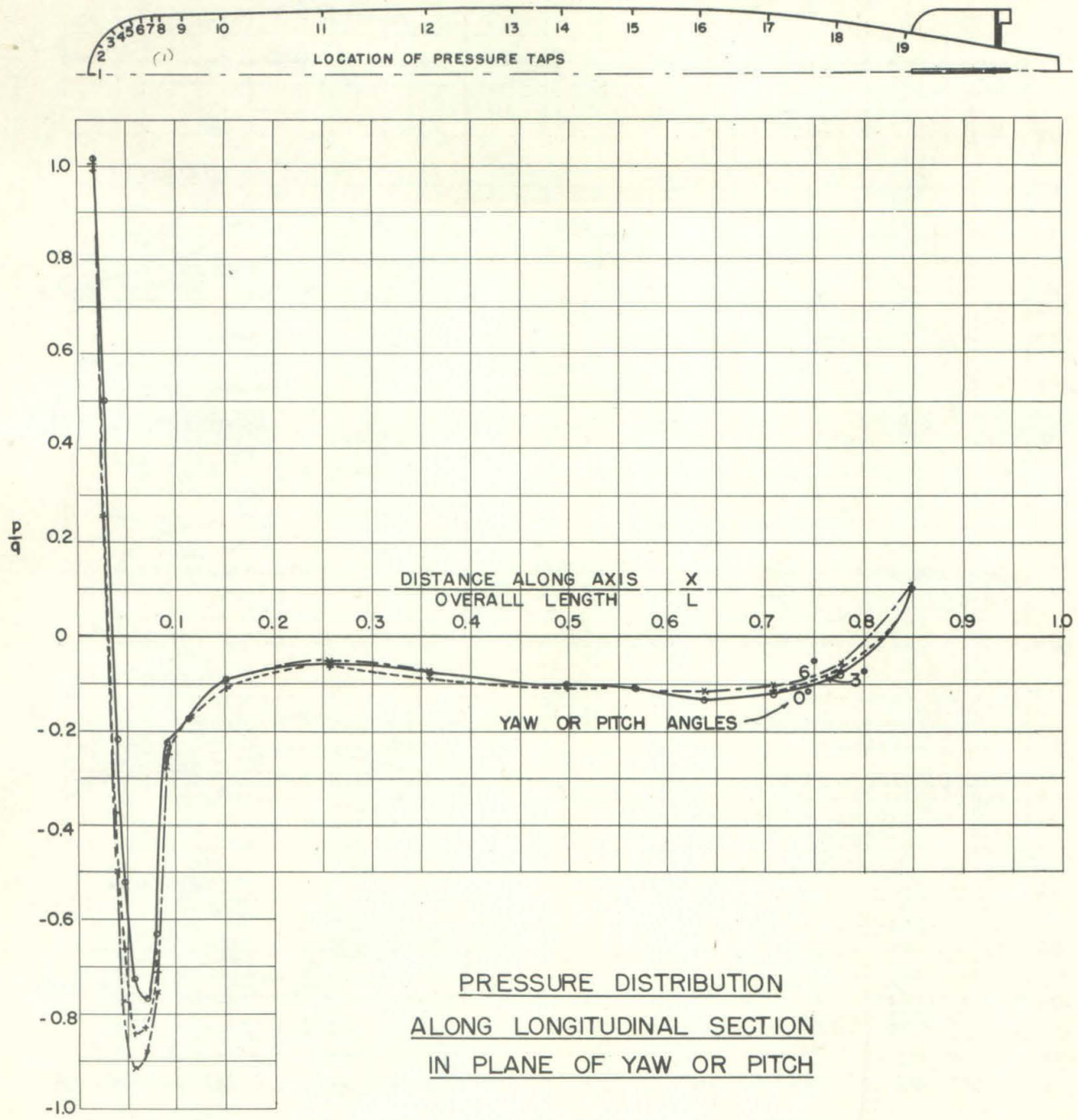

PRESSURE DISTRIBUTION
ALONG LONGITUDINAL SECTION
IN PLANE OF YAW OR PITCH

LEE SIDE OF BODY WITH FINS

CIT — HML
ND 15-3174 M

FIGURE 18

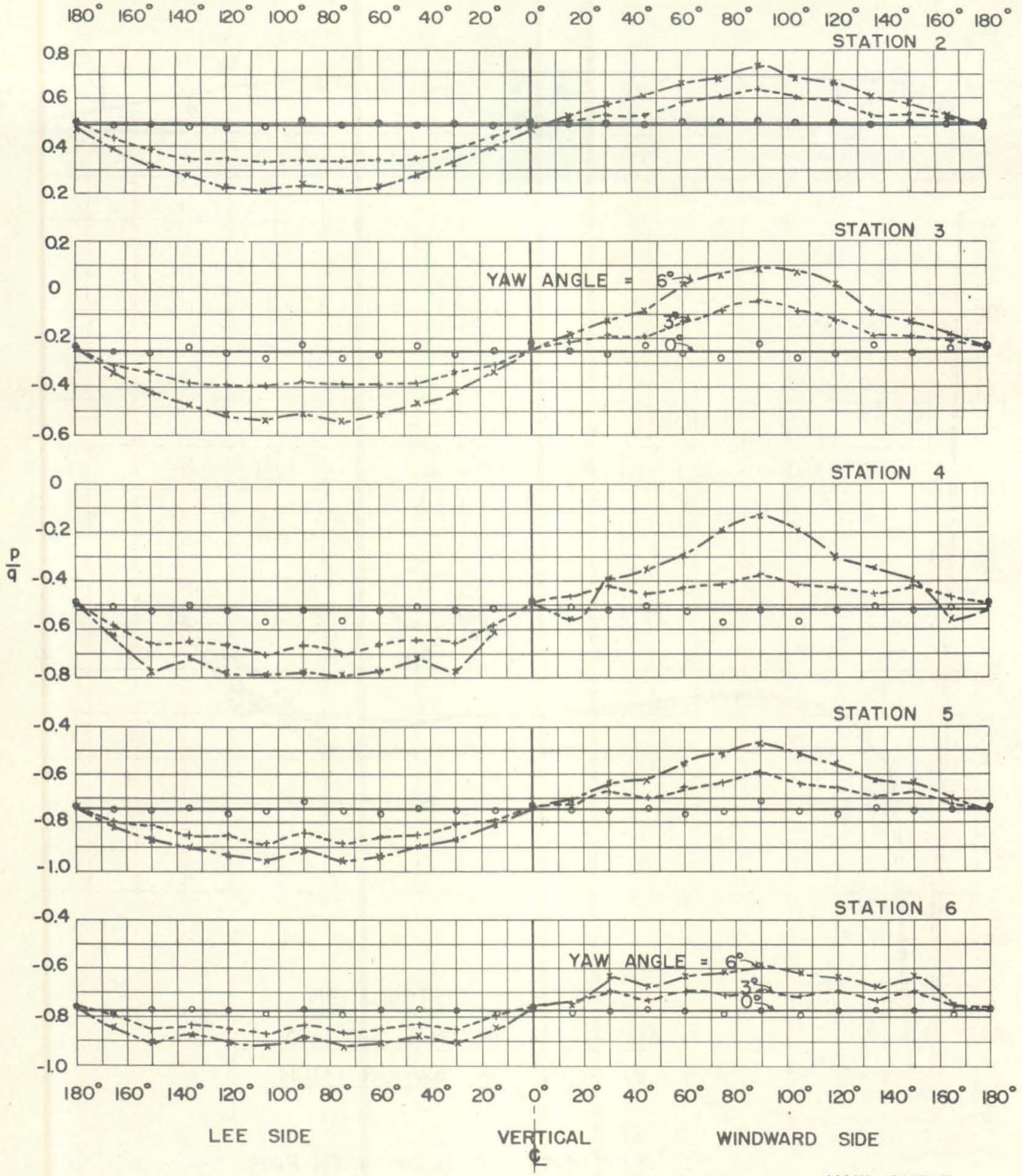

PRESSURE DISTRIBUTION ABOUT NORMAL CROSSECTION AT STATIONS ON FOREBODY

FIGURE 19

CIT – HML
ND 15-3175 M

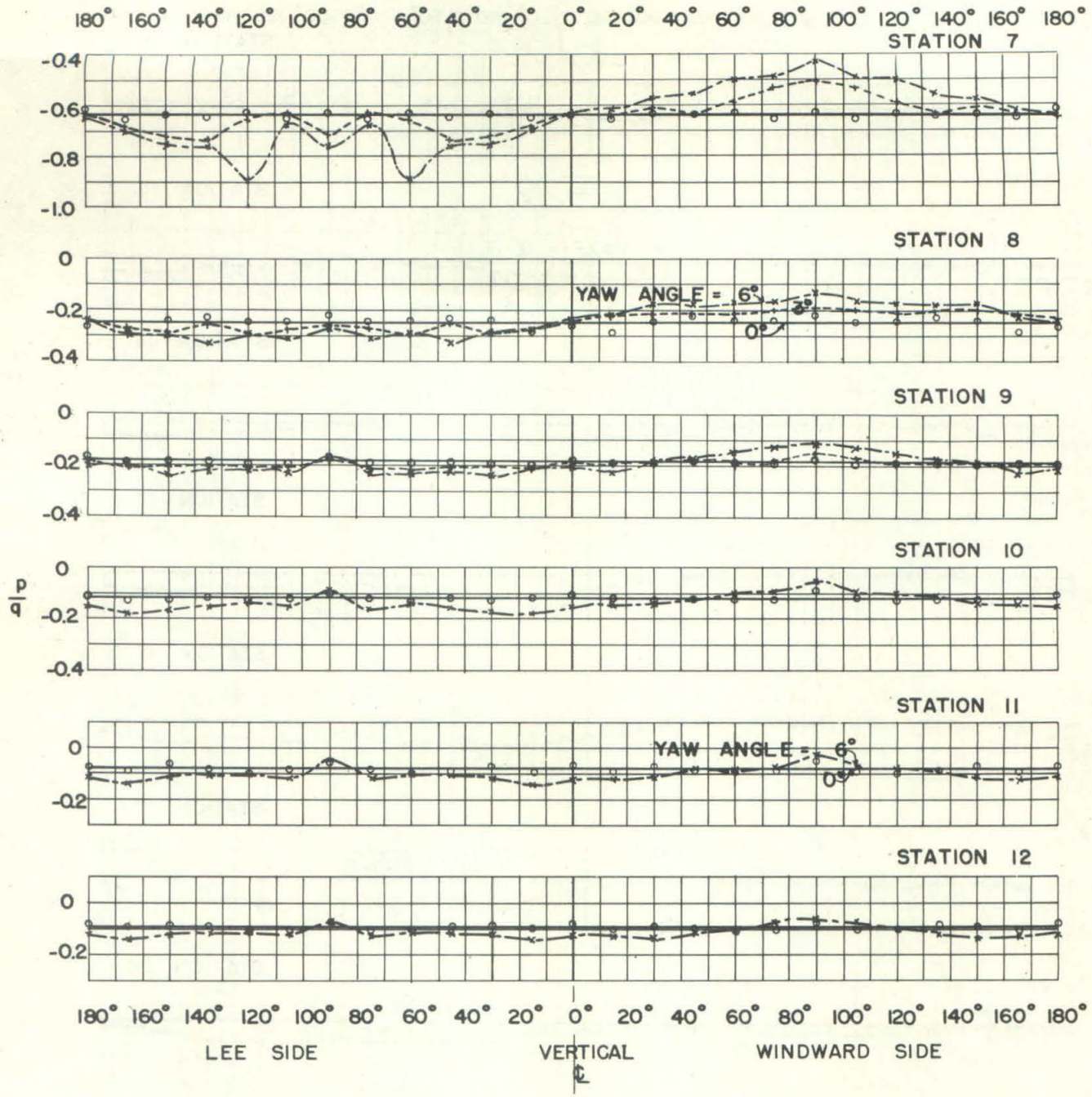

YAW ANGLE
- ○ 0°
- + 3°
- × 6°

PRESSURE DISTRIBUTION
ABOUT NORMAL CROSSECTION
AT STATIONS ON FOREBODY

CIT—HML
ND 15-3176 M

FIGURE 20

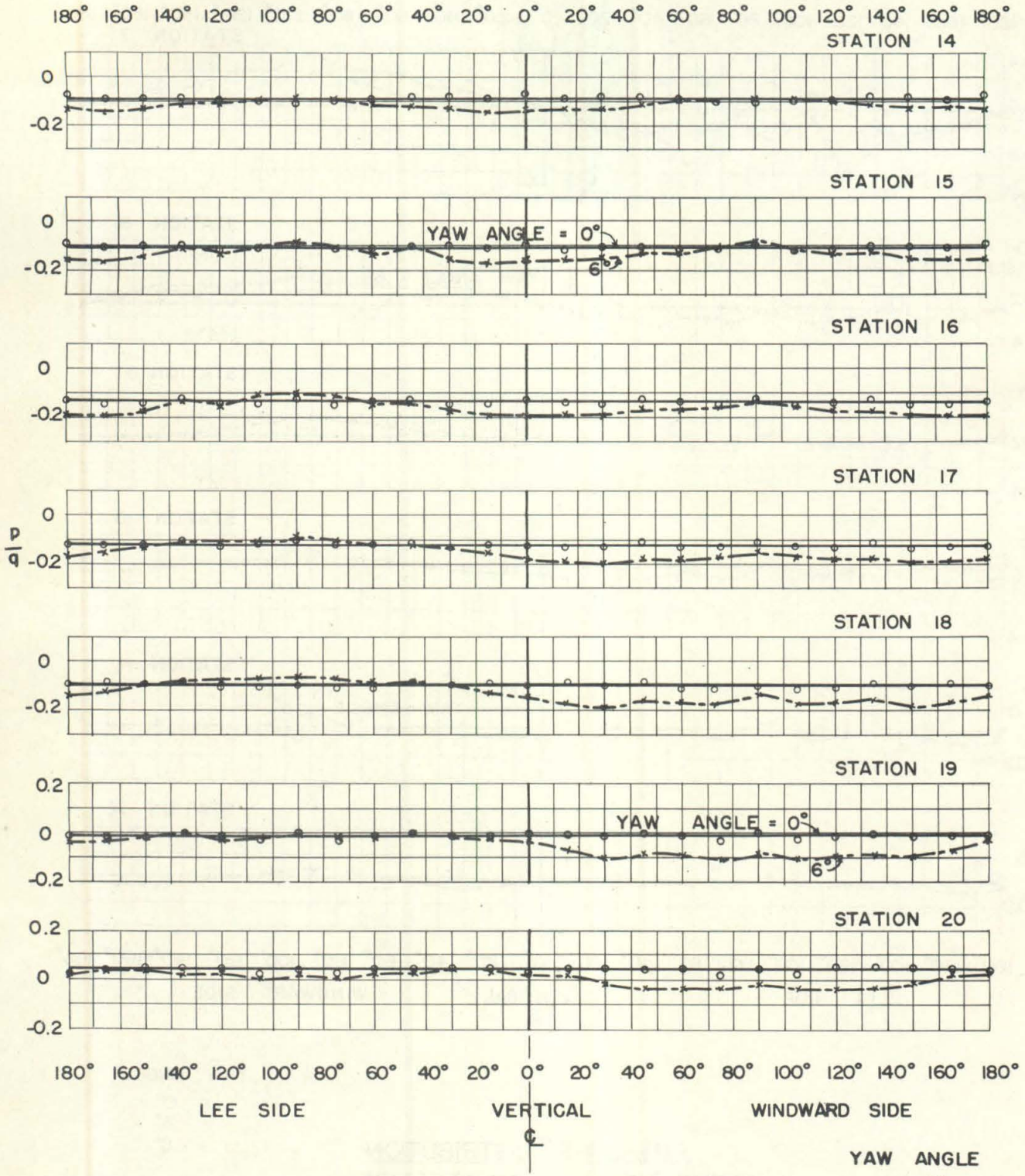

PRESSURE DISTRIBUTION
ABOUT NORMAL CROSSECTION
AT STATIONS ON AFTERBODY WITHOUT FINS

FIGURE 21

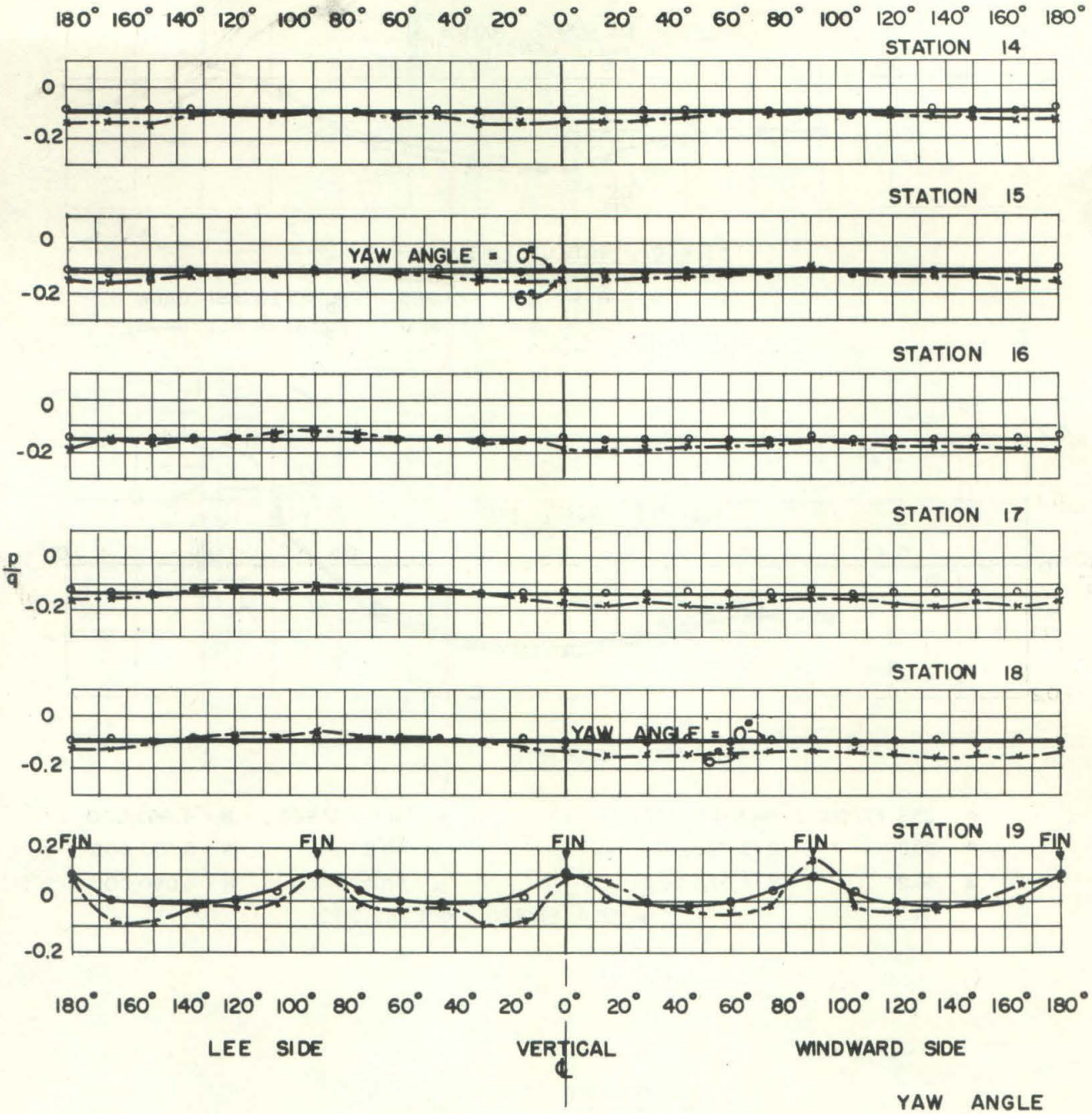

PRESSURE DISTRIBUTION ABOUT NORMAL CROSSECTION AT STATIONS ON AFTERBODY WITH FINS

CIT — HML
ND 15-3178 M

FIGURE 22

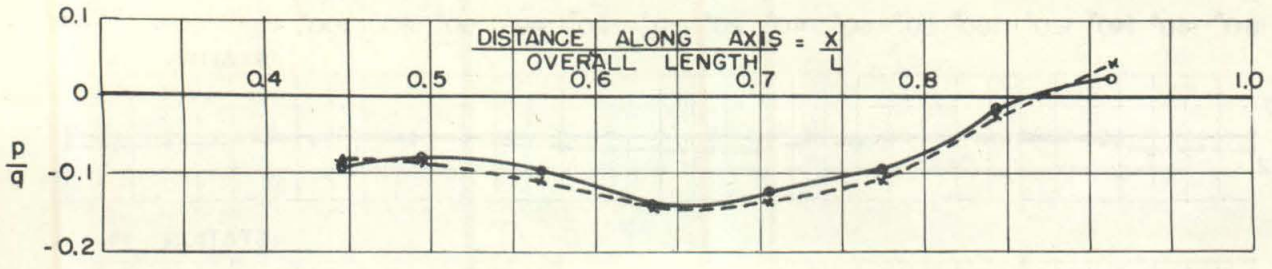

(a) BODY WITHOUT FINS

o 32.8 FT/SEC P_o = 20 PSI GAGE
x 32.8 FT/SEC P_o = 10 PSI GAGE

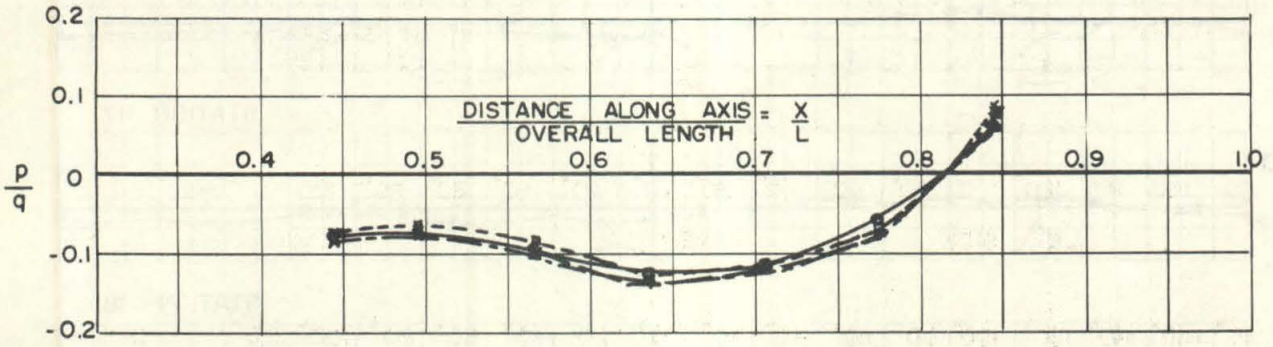

(b) BODY WITH FINS

o 25.8 FT/SEC , R = 3,120,000
▫ 30.8 " R = 3,728,000
▲ 36.2 " R = 4,375,000
▽ 41.1 FT/SEC , R = 4,960,000
+ 46.2 " R = 5,590,000
x 50.4 " R = 6,080,000
● 56.4 FT/SEC, R = 6,810,000

PRESSURE DISTRIBUTION ALONG TOP OF AFTERBODY

ZERO YAW

CIT — HML
ND 15-3179 L

FIGURE 23

IV. CAVITATION AND PRESSURE DISTRIBUTION

Cavitation, or the formation of vapor-filled cavities, occurs in hydraulic machinery or on underwater projectiles when the pressure at any point on the body becomes equal to the vapor pressure of the water. A knowledge of the pressure distribution around a projectile should, therefore, give an indication of the susceptibility of the projectile to cavitate. As defined in the preceding section, the data presented herein is given in terms of

$$\left(\frac{p}{q}\right) = \frac{P - P_o}{1/2\ \rho\ V^2}$$

In order to have cavitation, the pressure on the body, P, must equal the vapor pressure, P_v, or

$$P_v = P = \left(\frac{p}{q}\right)\ 1/2\ \rho\ V^2 + P_o$$

From the above equation, it is evident that cavitation cannot occur on the body at a point having a positive value of $\left(\frac{p}{q}\right)$, for then the static pressure P_o must be lower than P_v, and the entire volume of the liquid would boil. With a negative $\left(\frac{p}{q}\right)$, it is seen that, for a given water temperature (i.e., given P_v) cavitation conditions are approached as P_o is lowered or as V is increased. As cavitation is brought about, it will begin at that point on the body having the lowest value of $\left(\frac{p}{q}\right)$. Thus, the lowest value of $\left(\frac{p}{q}\right)$ measured on the body is an index of its susceptibility to cavitation, and is normally given as the cavitation parameter, K, which is defined by

$$K = \frac{P_o - P_v}{1/2\ \rho\ V^2}$$

Comparing this equation with the expression for $\left(\frac{p}{q}\right)$, it is seen that $K = -\left(\frac{p}{q}\right)_{min}$, i.e., the cavitation parameter for any shape is equal, but of opposite sign, to the lowest value of $\left(\frac{p}{q}\right)$ measured on that body.

The curves of Figures 7 and 8 indicate, therefore, that the inception of cavitation on these torpedoes should occur at a K value of 0.78, which is in good agreement with the results of cavitation tests made in the Water Tunnel.

The photograph of Figure 24 was used in Reference 1 to illustrate an early stage of cavitation, some time after inception, at a K value of 0.583. Referring to Figure 8 again, the cavitation should occur in the zone having $\left(\frac{p}{q}\right)$ values below -0.583, and that zone is seen to be just ahead of the junction of the hemispherical nose with the forebody taper. Figure 24 shows that cavitation

actually occurs at the zone just aft of this junction. It appears, therefore, that a definite time interval is required for the growth of a bubble to visible size, and during that time interval the bubble is carried downstream from its point of origin.

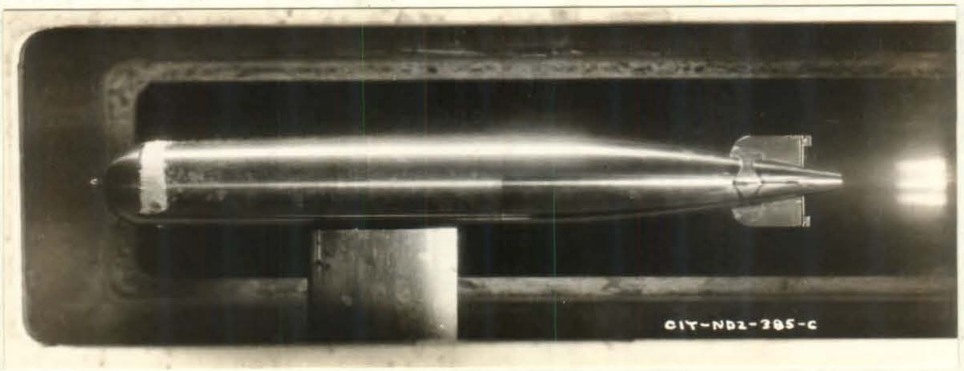

FIGURE 24

V. FORCES CALCULATED FROM PRESSURE DISTRIBUTION

With the pressure distribution around a projectile known, it is possible to calculate the form drag, cross force, and moment acting on the projectile. Since pressure measurements on the fins themselves were not made in these tests, it is possible only to calculate the forces acting on the bare hull. A comparison of several values thus calculated with those obtained from direct force measurements in the Water Tunnel is given below. The agreement between these two sets of data cannot be expected to be exact, since the evaluation of forces from pressure distribution data involves several graphical integrations of very small forces distributed over the entire surface of the body. The details of the steps involved in this calculation are given in Appendix C.

The pressure distribution data can be used to evaluate the form drag but not the skin friction drag. The drag actually measured in the tunnel consists of both form drag and skin friction drag. To compare these two, it is necessary, therefore, to evaluate the skin friction drag by some other means. This was calculated by the von Kármán logarithmic law for skin friction drag.

The form drag coefficient for zero yaw evaluated from pressure distribution was 0.025, as compared with 0.022 from force measurements. The cross force coefficient at 6° yaw from pressure distribution was found to be 0.40, from direct force measurements 0.55. The moment coefficient at 6° yaw evaluated from pressure distribution is 0.130 and from force measurements 0.112.

VI. LOCATION OF HYDROSTATIC PRESSURE INTAKE FOR DEPTH CONTROL

To enable the torpedo to travel at set depth under all conditions of speed and orientation with the direction of travel, it is necessary that the pressure intake to the hydrostat of the immersion (depth control) mechanism be located at a point where the pressure at the surface, under all conditions of speed and yaw or pitch, is equal to the static pressure in undisturbed water, that is, at a point where $\frac{p}{q}$ is equal to zero at all yaw or pitch angles. Also, the intake opening should be flush with the surface, at right angles to it, and with sharp square corners.

Behavior in Existing Location

The immersion mechanism on the torpedoes of the Mk 13 series are located in the afterbody at a point 38.6 inches ahead of the tail, where $\frac{X}{L}$ is approximately 0.76. An examination of the curves of Figures 9 to 18 shows that at that point the value of $\frac{p}{q}$ is not zero and that it varies with yaw and with pitch. It is evident, therefore, that these torpedoes cannot be expected to travel at set depth independent of angle or speed. Figure 10 shows that on the hull with fins at X/L = 0.76 and with zero yaw $\frac{p}{q}$ has a value of -0.1. That is, the pressure at that point is below static pressure by one-tenth of the dynamic pressure. The torpedo will tend, therefore, to travel below set depth. At a speed of 33.5 knots, this error in depth amounts to about five feet at zero yaw and to nearly 7 feet at 6° yaw.

Recommendations for Relocation

This can be corrected by sealing off the present intake to the immersion mechanism and connecting the hydrostat to a suitable piezometer opening or openings at another location. The longitudinal pressure distribution curves show that $\frac{p}{q}$ becomes zero at two locations along the torpedo, one at the nose and one on the afterbody ahead of the tail. The point on the nose may be eliminated as a possible location for pressure intake merely because of its distance from the immersion mechanism. This leaves the one other possible location, on the afterbody, a short distance aft of the immersion mechanism. Figures 13 and 14 show that for zero yaw $\frac{p}{q}$ becomes zero at X/L = 0.855, or 23.2" ahead of the tail. This point is just aft of the location of piezometer tap No. 19 of these tests. In Figure 22 is shown the pressure distribution around the body at this station for zero yaw and 6° yaw. It is seen that the pressure is high at the quadrant points (0, 90, and 180 degrees) because of the effect of the fins whose leading edges are just downstream of this station. Between the fins, the value of $\frac{p}{q}$ diminishes until it is about -0.01 at the 45 degree points, and at these points it is practically independent of yaw.

From the above discussion it appears that the best arrangement for an intake to the hydrostat would be through a piezometer ring connecting to four small openings on the 45° planes between the leading edges of the fins and about 23 inches ahead of the end of the tail.

Influence of Propellers

It should be noted that the tests reported herein were made on a model without propellers. The operation of the propellers on the prototype may modify the pressure distribution on the afterbody, so that the best location for the pressure intake may be slightly ahead or aft of the position indicated above.

Pressures with Shroud Ring Tails

It should be further noted here that the tests were made on models without shroud ring tails, and the results, therefore, apply to prototype torpedoes that have not been equipped with ring tails. Additional tests, on a model with the ring tail now being adopted, will be made in the near future and will be reported upon as soon as completed.

VII. LOCATION OF DEPTH AND ROLL RECORDER

Behavior in Existing Location

The depth and roll recorder used on these torpedoes in exercise runs is installed in one of the openings provided on the upper surface of the exercise head, some distance aft of the nose. The longitudinal pressure distribution curves show that in this region the pressure is lower than static. The depth and roll record, therefore, indicates a depth shallower than the actual running depth. As indicated in the preceding section, the location of the immersion gear is such as to cause the torpedo to run below set depth. With the torpedo running below set depth and carrying a depth and roll recorder which records a depth shallower than the actual running depth, it is possible to get a record which indicates a run at or near set depth when actually the torpedo ran several feet deeper.

Recommendations

This could probably be corrected by connecting the depth and roll recorder to piezometer openings on the nose where $\frac{p'}{q} = 0$. This, however, is not advisable because the pressure on the nose changes very abruptly, and because these tests were made with a model without the towing ring projection on the nose. The data presented herein may be used for estimating the correction to be applied to the depth record obtained with the recorder in its present location.

VIII. SUMMARY OF CONCLUSIONS AND RECOMMENDATIONS

The following paragraphs summarize the important information and conclusions obtained from the investigation of the pressure on the body of the Mk 13 Torpedo, Modifications 1, 2, and 2A.

First, the pressure measurements on the body with fin tail, but without shroud ring and without rotating propellers gave the following characteristics:

1. The pressure on the surface of the torpedo body equals the static pressure corresponding to the running depth or submergence at two positions, one on the projectile nose and one on the afterbody. (See Figure 8). Ahead and behind these two stations the pressure is above static, while between the two (which includes about 82% of the body length) the pressure is below static.

2. The presence of fins on the afterbody causes local high-pressure zones in their immediate vicinity, but produces no appreciable effect on the pressure midway between the fins. (Compare Figures 21 and 22, Station 19). Consequently, the points where $P = P_o$ on the afterbody depend on the proximity of the fins. The fins do not influence the pressure over the nose or forward part of the projectile body. (Compare Figures 7 and 8).

3. The position on the afterbody at which $P = P_o$ is only slightly affected by yaw or pitch angles up to 3^o. (See Figures 13, 14, 17, and 18).

4. The measured pressure distributions are unaffected by changes in velocity or static pressure (submergence). (See Figure 23).

Second, the application of the above characteristics to the problems of depth control and depth recording lead to the following conclusions and recommendations:

5. The existing location of the pressure intake for depth control (to the immersion gear) gives a pressure lower than the true hydrostatic pressure at the torpedo centerline and causes the torpedo to ride below set depth by an amount depending on yaw, pitch, and velocity.

6. On the basis of these measurements without a rotating propeller, true hydrostatic pressure, independent of velocity and of small yaw or pitch angles, will be obtained if the pressure connections to the immersion gear are located midway between the tail fins and about 23 inches ahead of the tip of the tail. The influence of the propeller may shift this point slightly.

7. The depth and roll recorder is so located in the exercise head of this torpedo, that the pressure measured is less

than the true hydrostatic. With the depth control gear forcing the projectile to lower than set depths as described in (5) above, the recorder may indicate approximately set depth for runs that are actually several feet too deep.

8. Placing the pressure take-off for the depth recorder where $P = P_o$ on the nose is not recommended because P changes rapidly in this zone and large errors can result from small inaccuracies in locating the connection. Taking the pressure from the afterbody is not feasible because of the physical obstructions inside the torpedo. It is recommended that the data reported here be used to estimate corrections to apply to the recorder used in its present location.

Finally the use of the pressure measurements to evaluate the hydrodynamic forces and moments and to estimate the projectile's susceptibility to cavitation and the probable location of cavitation give the following results:

9. The form drag and moment coefficients calculated from the pressure distribution data are about 15% higher than given by Water Tunnel measurements. The calculated cross force coefficient is 27% lower than measured.

10. The inception of cavitation should occur when $K = -\left(\frac{p}{q}\right) = 0.78$, which is in good agreement with the results of cavitation tests made in the Water Tunnel.

11. As observed in the tunnel, cavitation actually becomes visible at a point aft of the position where minimum pressure is indicated by the measurements on the body. This may be caused by a true lag between the water entering into the low pressure environment and its actual vaporizing to give a bubble that can be seen.

It should be emphasized that these measurements were made with the standard ringless tail and that the above conclusions regarding pressures over the afterbody apply only to torpedoes without rings. Additional measurements on a model with the ring tail are being made and will be submitted in another report.

APPENDIX A

TEST EQUIPMENT AND PROCEDURES

The tests covered by this report were conducted in the High Speed Water Tunnel at the California Institute of Technology. The following paragraphs contain a brief description of the tunnel and the test procedures employed. A more detailed description of the High Speed Water Tunnel will be found in Reference 4.

MAIN CIRCUIT

The Water Tunnel is of the closed circuit, closed working section type. Figure A-1 shows a profile of the main flow circuit which consists essentially of the working section, the circulating pump, the stilling tank, and the necessary pipe connections. The cylindrical working section is 14" in diameter, 72" long, and is provided with three lucite windows. The propeller-type circulating pump is V-belt connected to a variable speed dynamometer. The speed of the dynamometer is automatically controlled and is held constant within ± 1 r.p.m., which corresponds to a maximum water velocity variation in the working section of 1/30 ft. per sec. While most tests are made with water velocities of 24 to 31 ft. per sec., any velocity between 10 and 72 ft. per sec. is easily obtainable.

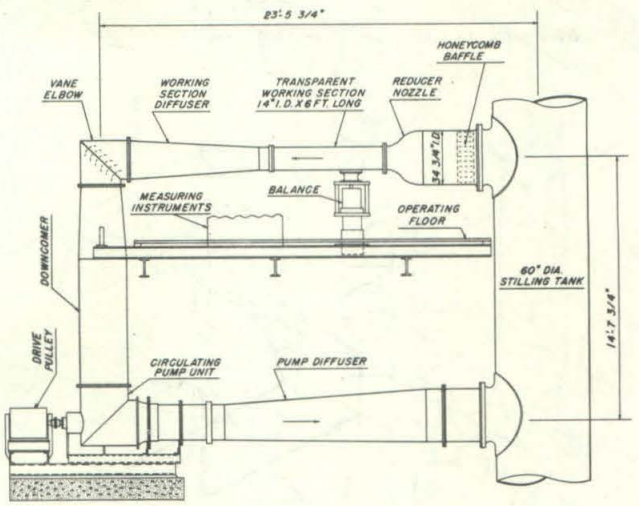

FIGURE A-1

AUXILIARY CIRCUITS

Two auxiliary water circuits, one for pressure control and one for temperature control, are used in conjunction with the main circuit. These circuits are shown in Figure A-2, which is an isometric diagram of the complete water tunnel installation.

To make it possible to induce or inhibit cavitation at will, it is necessary that the pressure in the working section be controllable independently of the velocity. This is accomplished by superimposing the pressure regulating circuit on the main circuit.

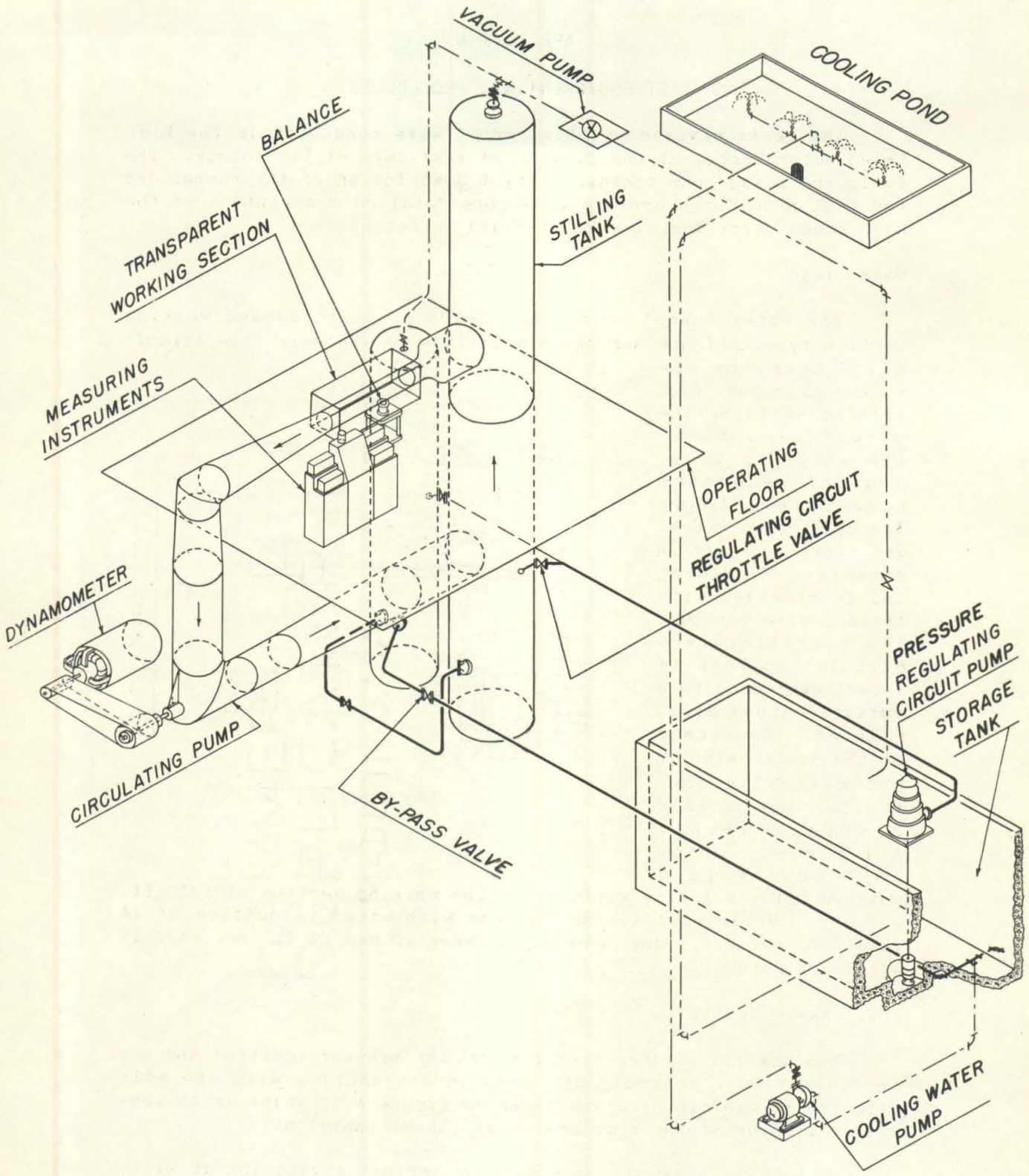
VACUUM PUMP
COOLING POND
BALANCE
TRANSPARENT WORKING SECTION
STILLING TANK
MEASURING INSTRUMENTS
OPERATING FLOOR
REGULATING CIRCUIT THROTTLE VALVE
DYNAMOMETER
PRESSURE REGULATING CIRCUIT PUMP
STORAGE TANK
CIRCULATING PUMP
BY-PASS VALVE
COOLING WATER PUMP

FIGURE A-2

A small flow of water from the sump is forced into the stilling tank by the regulating pump, and is returned to the sump through the by-pass valve. Since the main circuit is closed and completely filled, it is evident that the pressure in it may be controlled by varying the opening of the by-pass valve. A stripping pump (not shown in Figure A-2), in series with the by-pass valve, is used to produce very low pressures. The vacuum pump is used to remove air from the system so as to keep it full of water at all times.

The energy put into the water of the main circuit by the circulating pump (up to 250 HP) is all dissipated in heat. To prevent the temperature of the water from rising to undesirable values, it is necessary to remove this heat by cooling. Part of the water returned through the by-pass valve is picked up by the cooling water pump, circulated through the forced-draft cooling tower on the roof, and returned to the sump. By varying the quantity of water circulated through the cooling system, it is possible to maintain the water in the main circuit at a constant temperature.

BALANCE

The balance, shown schematically in Figure A-3, is designed to measure three components of the hydrodynamic forces acting on the model. These are the drag force parallel to the flow, the cross force normal to the flow, and the moment around the axis of support. The three forces to be measured are transmitted hydrostatically to three self-balancing, weighing type pressure gages. These automatic gages, under glass covers, may be seen in Figure A-4, which is a view of the operating floor of the Water Tunnel. The fourth gage shown in this figure is a weighing type manometer used to determine the velocity in the working section by measuring the pressure drop across the reducing nozzle. The gages are responsive to a change in the drag or cross force acting on the model of 0.02 pounds, and a change of 0.04 inch-pounds in the moment.

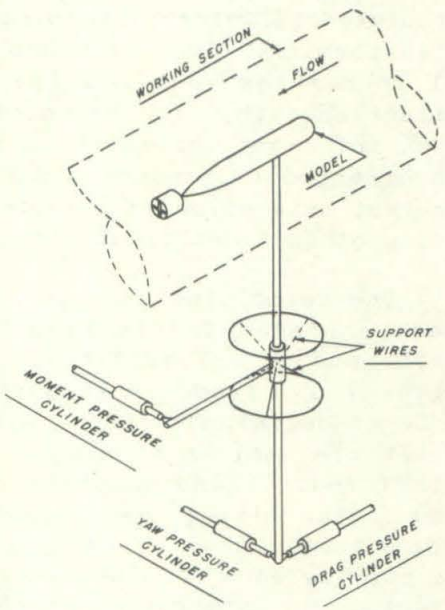

FIGURE A-3

The model is mounted on a shaft which forms the core of the vertical balance spindle shown in Figure A-3. By rotating this shaft within the spindle, it is possible to change the orientation of the model with respect to the direction of flow without altering the direction of the force components measured. Between adjustments, the spindle and shaft are held firmly together by a long, spring-loaded, tapered seat. To change the adjustment, the taper is unseated by an air diaphragm and the shaft is rotated through a worm and gear-sector by a small electric motor (not shown in the figure) mounted on the spindle. A Veeder counter on the worm gear shaft indicates the angle of attack to the nearest 1/10 degree. It should be noted that this whole system forms a part of the spindle assembly, which is pivoted about the point of intersection of the support wires. Thus it does not affect the force measurements in any way.

To reduce the drag tare to a minimum, the portion of the spindle shaft which projects into the working section is protected from the flow by a streamlined shield which extends to within a few thousandths of an inch of the model.

POLARIZED LIGHT FLUME

The Polarized Light Flume is a separate piece of equipment used for studying the flow around submerged bodies. The fluid circulated is water containing 0.2 per cent by weight of Bentonite in suspension. Bentonite has the asymmetrical optical and physical properties required for the production of streaming double refraction. The flow to be studied is made visible by projecting a beam of light across it through a pair of polaroid plates which are oriented to produce a dark field when there is no flow. The observation section is a rectangular channel 6" wide and 12" deep, having glass sides and bottom.

The velocities used in this flume are necessarily lower than those employed in the High Speed Water Tunnel. However, this difference is not sufficient to affect the validity of the flow patterns observed. A knowledge of these flow patterns is found to be of assistance in the interpretation of the dynamic behavior of the projectiles studied. It is very helpful in investigating interference phenomena, the cause and location of separation or flow instabilities, and the behavior of the boundary layer. Care must be exercised in interpreting the observed patterns, both because the flow is three-dimensional, whereas the observed optical effect is an integration of the entire path of the light beam, and because the pattern produced is a shear pattern and not one of streamlines.

TEST PROCEDURES

The facilities of the High Speed Water Tunnel provide for great flexibility in operation and test procedures. Individual test runs are usually made to determine the effect on the hydrodynamic forces of individual variables, although any of the variables may be changed at will independently of the others.

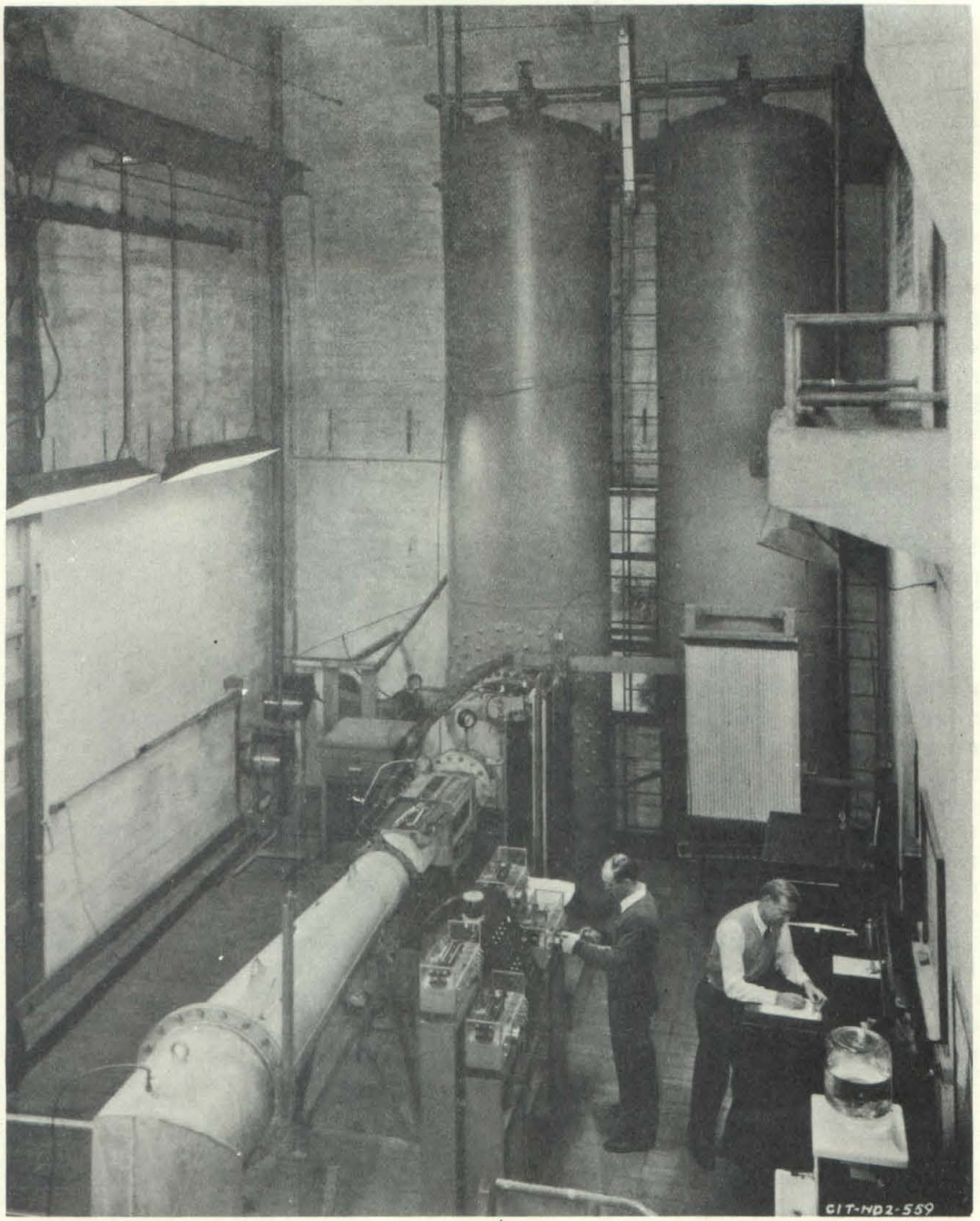

FIGURE A-4

OPERATING FLOOR
OF THE
HIGH SPEED WATER TUNNEL

Constant-velocity tests runs are made to determine the variation of the hydrodynamic forces with changes in the orientation of the projectile with respect to the line of flow. The angle of attack is changed in steps of 1/2 or 1 degree, and the three force components are measured at each step.

A single test, covering the desired range of angles of attack is sufficient to completely determine the yawing characteristics of a projectile which is symmetrical about its longitudinal axis and has no movable control surfaces. A projectile which is not symmetrical about its longitudinal axis (e.g., having unequal horizontal and vertical fins) will show different characteristics when yawed in different planes and, therefore, must be tested in more than one plane. Since the model can be yawed only in a plane normal to the spindle, this is accomplished by making several separate test runs, with the model mounted on the spindle in a different orientation for each run. For instance, one run with vertical fins in a vertical position and another with horizontal fins in a vertical position. These would correspond to a yawing test and a pitching test, respectively. For a projectile with movable rudders, several tests are made, each with the rudders set at a different angle.

Cavitation is an important factor in the behavior of underwater projectiles travelling at high speed near the surface. To determine the cavitation characteristics of such a projectile, separate tests are made during which the pressure is varied while all the other factors are held constant. The inception and development of cavitation may be observed or photographed through the transparent windows of the working section, and the velocities and pressures at which cavitation begins on the various parts of the projectile are measured.

Variable-speed test runs are made to determine the scale (Reynolds number) effect on the hydrodynamic forces. The speed is usually varied in 5 fps steps and the forces are measured at each step. The pressure in the working section is kept high enough to suppress cavitation at the highest velocity.

APPENDIX B

DEFINITIONS

PITCH ANGLE

The angle in the vertical plane which the axis of the projectile makes with the direction of travel. Pitch angles are positive (+) when the nose is up, and negative (-) when the nose is down.

YAW ANGLE

The angle in the horizontal plane which the axis of the projectile makes with the direction of travel. Looking down on the projectile and in the direction of travel, yaw angles to the right are positive (+), and to the left, negative (-).

LIFT

The force, in pounds, exerted on the projectile in a direction normal to the line of travel and in the vertical plane, positive (+) when acting upward, and negative (-) when acting downward.

CROSS FORCE

The force, in pounds, exerted on the projectile in a direction normal to the line of travel and in the horizontal plane. A positive cross force is defined as one acting in the same direction as the displacement of the projectile nose for a positive yaw angle.

DRAG

The force, in pounds, exerted on the projectile in a direction parallel with the line of travel. The drag is positive when acting in a direction opposite to the direction of travel.

MOMENT

The torque tending to rotate the projectile about a transverse axis. A positive or clockwise moment tends to increase a positive yaw or pitch angle. A moment, therefore, has a destabilizing effect when it has the same sign as the yaw or pitch angle, and a stabilizing effect when of opposite sign.

COEFFICIENTS

The force and moment coefficients are defined as follows:

Lift Coefficient, $$C_L = \frac{L}{1/2\ \rho\ V^2 A}$$

Cross Force Coefficient, $$C_C = \frac{C}{1/2\ \rho\ V^2 A}$$

Drag Coefficient, $C_D = \frac{D}{1/2\ \rho\ V^2 A}$

Moment Coefficient, $C_M = \frac{M}{1/2\ \rho\ V^2 A l}$

where

L = lift force, pounds

C = cross force, pounds

D = drag force, pounds

M = moment, foot-pounds

ρ = density of water, slugs per cu. ft.

V = velocity, feet per second

A = area of a crossection taken normal to the longitudinal axis of the projectile at its maximum diameter, square feet

l = overall length of projectile, feet

REYNOLDS NUMBER $R_e = \frac{Vl\rho}{\mu} = \frac{Vl}{\nu}$

where

V, l, and ρ are as defined above, and

μ = absolute viscosity of water, pound-second per square foot

$\nu = \frac{\mu}{\rho}$ = kinematic viscosity of water, square feet per second

CAVITATION PARAMETER $K = \frac{P_o - P_V}{1/2\ \rho\ V^2}$

where

ρ and V are as defined above, and

P_o = absolute pressure in undisturbed water, pounds per square foot

P_b = pressure in the cavitation bubble (usually taken as the vapor pressure of the water), pounds per square foot

APPENDIX C

CALCULATION OF FORCES AND MOMENTS FROM PRESSURE DISTRIBUTION DATA

The following paragraphs describe the method of calculating form drag, cross force, and moment acting on the projectile from measured pressures on its surface.

CROSS FORCE

The normal force, n, per foot of projectile length, acting on a vertical plane which contains the longitudinal axis of the body, at any station is given by

$$(1) \qquad n = \frac{dN}{dX} = \int_0^{2\pi} P\, r \sin\phi\, d\phi$$

$$= 1/2\ \rho\ V^2\ r \int_0^{2\pi} C_p \sin\phi\, d\phi$$

where in addition to the terms defined by the accompanying figure

P = local pressure on the body surface

$$C_p = \frac{P}{1/2\ \rho\ V^2}$$

Because of symmetry, equation (1) can be written as

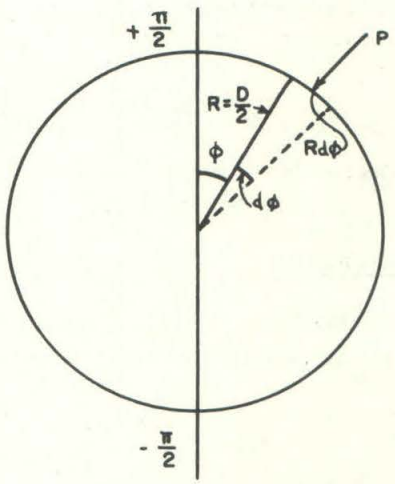

CROSSECTION NORMAL TO PROJECTILE AXIS

$$(2) \qquad n = 1/2\ \rho\ V^2 d \int_{-\frac{\pi}{2}}^{\frac{\pi}{2}} C_p \sin\phi\, d\phi$$

This is readily solved using the measured values of P and integrating graphically.

The total normal force acting on the body is given by

(3) $$N = 1/2\ \rho\ V^2 \int_0^L S_n\ dX$$

where

$S_n = \frac{n}{1/2\ \rho\ V^2}$ is evaluated from equation (2) for each measuring station

X = distance from nose to station

L = overall length of projectile

Using this value of N, which is obtained by graphical integration also, the normal force coefficient becomes

(4) $$C_N = \frac{N}{1/2\ \rho\ V^2 A} = \frac{\int_0^L S_N\ dX}{A}$$

Assuming small yaws so that contributions from the longitudinal pressure force component can be neglected, the cross force coefficient is

(5) $$C_c = C_N \cos \psi$$

which is approximately $C_c = C_N$

FORM DRAG

The longitudinal pressure force can be set equal to the form drag for small yaw angles. It is expressed as

(6) $$D = \int_{nose}^{tail} PdA = 1/2\ \rho\ V^2 \int_{nose}^{tail} C_p\ dA$$

A = the area of the cross section of the body at each measuring station

P = the average pressure around the body at each station

$$C_p = \frac{P}{1/2\ \rho\ V^2}$$

After evaluating graphically, the form drag coefficient becomes

(7) $$C_D = \frac{D}{1/2\ \rho\ V^2\ A}$$

MOMENT

The moment about the center of gravity due to the normal force is given approximately by

$$(8) \qquad M = 1/2\ \rho\ V^2 \int_o^L S_N\ y\ dX$$

where y = distance of any station from the C.G.

This neglects any contribution from the drag component and, hence holds only for small yaw angles. Again equation (8) is integrated graphically.

The moment coefficient is

$$(9) \qquad C_M = \frac{M}{1/2\ \rho\ V^2\ AL}$$

APPENDIX D

REFERENCES:

(1) "Water Tunnel Tests of the Mk 13-1, Mk 13-2, and Mk 13-2A Torpedoes," Section No. 6.1-sr207-936, November 9, 1943.

(2) "Water Tunnel Tests of the Mk 13-1, Mk 13-2, and Mk 13-2A Torpedoes with Shroud Ring Tails," Section No. 6.1-sr207-939, November 24, 1943.

(3) "Water Tunnel Tests of the Mk 13 Torpedo with Spade and Stabilizer Ring Noses," Section No. 6.1-sr207-1278, May 30, 1944.

(4) "The High Speed Water Tunnel at the California Institute of Technology," June 29, 1942.